and middle). On the other hand, another monkey, Mf-3, which had higher proviral load (17%), possessed two major STLV-1-infected clones (Figure 6A, right). To study which cell types are infected by STLV-1, Tax expression in PBMCs obtained from one monkey (Mf-4) was analyzed by flow cytometry. The Tax-expressing cells were largely found to be $CD4^+$ T cells, as is the case with HTLV-1 infection in humans (Figure 6B).

STLV-1-associated T-cell lymphoma in a Japanese macaque

A monkey (Mf-4) developed anorexia and had paralysis of the lower limbs. This monkey had high proviral load (53%) in PBMCs. We suspected that this monkey has developed a disease similar to HAM/TSP because paralysis of the lower limbs is one of the major symptoms of HAM/TSP patients. Magnetic resonance imaging (MRI) revealed a high intensity lesion in the brain on a T2-weighted image (Figure 6C). Pathological analysis showed that this tumor was a lymphoma with atypical morphology, and by immunohistochemical methods, it was found that these cells were $CD3^+$ $CD4^+$ (Figure 6D). In contrast, no obvious demyelination was observed in the spinal cord. Thus, this monkey was diagnosed with T-cell lymphoma in the brain rather than the disease like HAM/TSP. In this monkey, some major clones had proliferated in peripheral blood (Figure 6E, left). We found that the major clones in peripheral blood were also detected in the brain lesion (Figure 6E, right). These observations demonstrate that STLV-1 causes lymphoma in Japanese macaques. Notably, one of the major clones in the brain, which had its provirus integration site in chromosome 13, was not detected in PBMCs. This was confirmed by conventional PCR using the primers for the 3'LTR and the host genome proximal to the integration site (Figure 6F). Moreover, a clone with the integration site in chromosome 18 was also detected only in the brain lesion. These tumor-specific

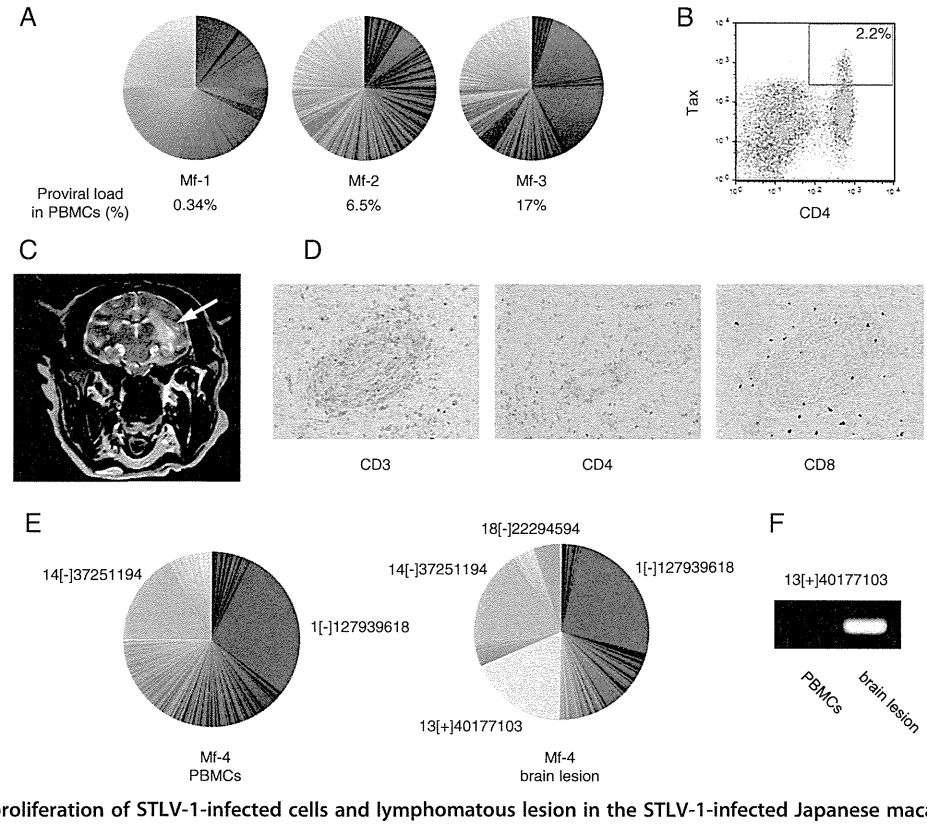

Figure 6 Clonal proliferation of STLV-1-infected cells and lymphomatous lesion in the STLV-1-infected Japanese macaque. (A) The relative frequency of STLV-1^+ clones in three monkeys (Mf-1, Mf-2 and Mf-3) is presented. Each area in the pie charts represents the proportion of provirus in a separate clone (identified by its unique integration site). **(B)** Flow cytometric analysis of PBMCs from an STLV-1-infected monkey shows that Tax-expressing cells are positive for CD4. **(C)** Magnetic resonance imaging of the brain of monkey Mf-4. The lesion is indicated by the white arrow. **(D)** Immunohistochemical analyses show that lymphoma cells are positive for CD3 and CD4. **(E)** Relative abundance of STLV-1^+ clones identified by unique integration sites of the provirus in PBMCs (left) and in the brain lesion (right) of Mf-4. Some of the abundant clones that are observed both in PBMCs and the brain lesion are painted in the same color in the two pie charts. **(F)** STLV-1^+ abundant clone 13[+] 40177103 is detected in the brain lesion by using the primers for 3' LTR and the genomic region, but not in PBMCs.

STLV-1-infected clones are thought to contribute to the formation of the tumor.

Treatment with anti-CCR4 antibody decreased proviral load in STLV-1-infected Japanese macaques

ATL cells express high levels of CC chemokine receptor 4 (CCR4) [28]. Recently, mogamulizumab, a humanized IgG1 monoclonal antibody against CCR4 [29], was approved in Japan for the treatment of relapsed ATL patients. HTLV-1-infected cells of healthy carriers also express CCR4, which indicates that mogamulizumab likely reduces the proviral load in HTLV-1-infected asymptomatic individuals [30]. High proviral load has been reported to be associated with HAM/TSP, HTLV-1 uveitis, and risk of ATL, indicating that mogamulizumab may potentially be used for the treatment of HTLV-1-associated diseases and the prevention of ATL. However, it is not clear whether mogamulizumab can reduce the proviral load in HTLV-1-infected individuals. We confirmed that mogamulizumab also recognizes macaque CCR4 by staining Japanese macaque PBMCs *in vitro* with the fluorescently labeled antibody (see Additional file 3). Then, we tested the efficacy of mogamulizumab to reduce the proviral load in STLV-1-infected Japanese macaques. Mogamulizumab was administered to two monkeys with high proviral load (Mf-6 and Mf-7), once a week for 4 weeks. As shown in Figure 7A, nearly half of the $CD4^+$ T cells expressed CCR4 before the treatment (week 0). After the treatment, the CCR4 positivity decreased to 1.62% and 12.4% respectively. We also

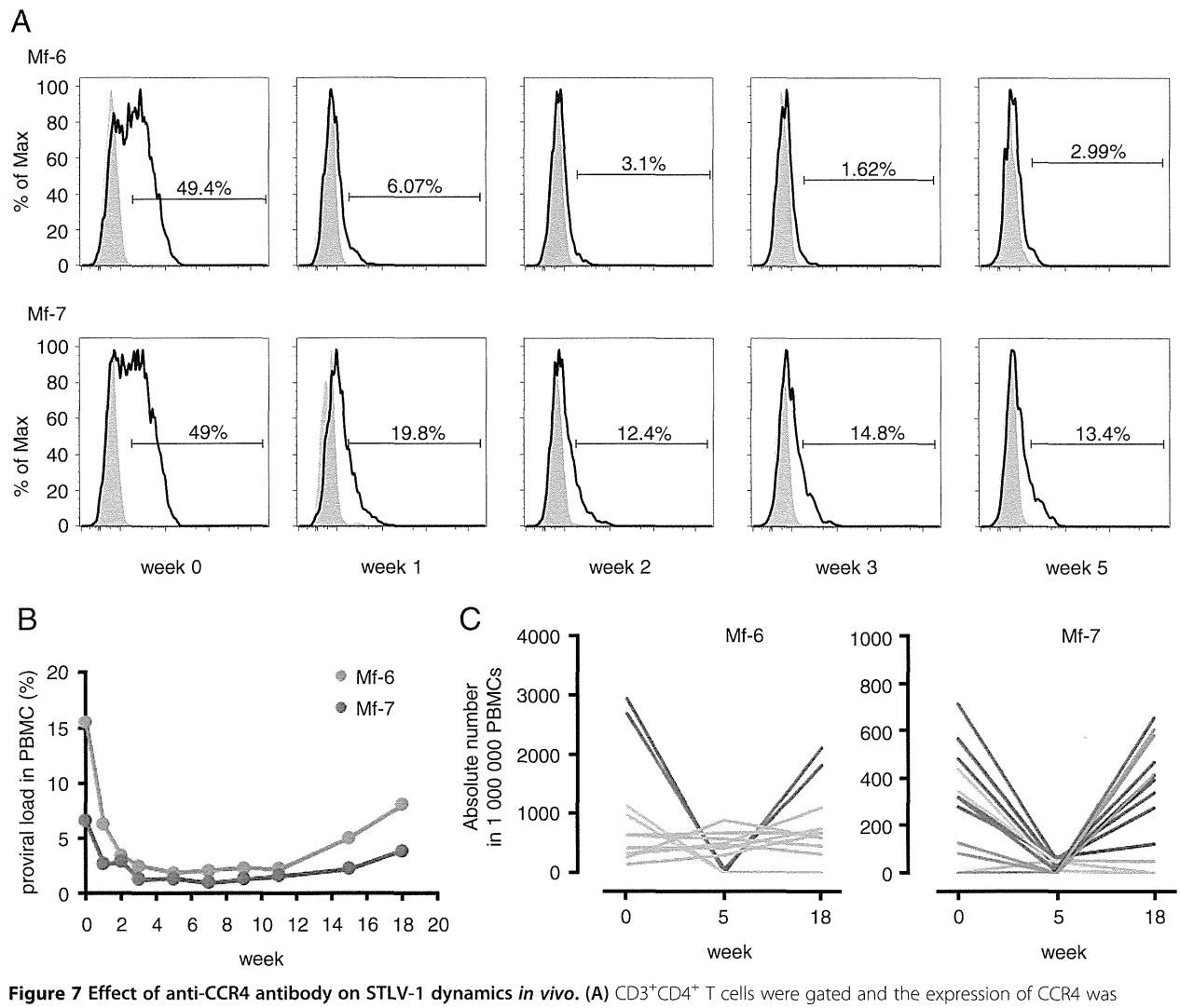

Figure 7 Effect of anti-CCR4 antibody on STLV-1 dynamics *in vivo*. **(A)** $CD3^+CD4^+$ T cells were gated and the expression of CCR4 was analyzed by flow cytometry. **(B)** Changes in STLV-1 proviral load in two monkeys treated with anti-CCR4 antibody until week 3. **(C)** Absolute cell numbers of the five most abundant clones in 1,000,000 PBMCs at weeks 0, 5 and 18 are shown.

measured proviral load over the course of the treatment and found that it decreased dramatically within 2 weeks (Figure 7B). Thus, this demonstrates that mogamulizumab can indeed reduce the number of STLV-1-infected cells *in vivo*.

Eight weeks after the final administration of mogamulizumab, the proviral load started to recover (Figure 7B). To investigate whether mogamulizumab influences the clonality of STLV-1-infected cells, we evaluated the absolute number of each clone by high-throughput sequencing of provirus integration sites. Figure 7C shows changes of the five most abundant clones at weeks 0, 5 and 18. The major clones before the treatment (week 0) recovered at week 18 (red lines in Figure 7C), while some clones were present constantly during the treatment (grey lines) or diminished after the treatment (blue lines). Interestingly, some clones (green lines) that emerged in a monkey after treatment were rare or even not detected before treatment (Figure 7C).

Discussion

HTLV-1 is thought to originate from STLV-1. In STLV-1-infected monkeys, investigators found clonal proliferation of STLV-1-infected cells and the preferential infection of $CD4^+$ T cells by the virus [15,31]. Moreover, several groups reported the development of lymphomas in STLV-1-infected monkeys [16,17,32-35]. Monoclonal integration of STLV-1 in the lymphoproliferative disease of African green monkeys was detected by Southern blot [16,33], demonstrating the direct causative role of STLV-1. Thus STLV-1-infected non-human primates have been thought to be a useful animal model for HTLV-1 research. The dynamics of infected cells after treatment with histone deacetylase inhibitors and reverse transcriptase inhibitors has been analyzed in STLV-1-infected baboons, and it was found that this combination significantly decreased proviral load in treated animals [36]. However, there have been no detailed studies on functions of STLV-1-encoded genes. Analyses of the functions of its accessory and regulatory proteins are necessary if we are to use STLV-1-infected monkeys as a model of HTLV-1 infection. In the present study, we focused on Japanese macaques naturally infected with STLV-1.

The amino acid sequence of STLV-1 Tax is closely homologous to that of HTLV-1 Tax, and this study demonstrated that their functions on various transcriptional pathways are similar as well. This study was the first to identify SBZ as an antisense transcript of STLV-1 and a homolog of HBZ. SBZ and HBZ share only approximately 73% identity at the amino acid level. Nevertheless, for all the functions we examined, SBZ behaves similarly to HBZ. In particular, SBZ expression could induce Foxp3 expression like HBZ expression does. This might be attributed to the following reasons. First, the N-terminal region, as well as the heptad repeats of hydrophobic amino acids in the basic leucine zipper domain, are conserved between HBZ and SBZ. This may allow SBZ to interact with and suppress NF-κB, AP-1 and other transcription factors with basic leucine zipper motifs [37,38]. Second, the LXXLL-like region (Leu27, Leu28, Leu48 and Leu49), which is critical for the interaction with p300 and Smad3 protein, is also conserved between HBZ and SBZ [22,39]. Some lysine residues present in HBZ are substituted with different amino acids in Japanese macaque SBZ. This study showed that SBZ has similar functions compared with HBZ, suggesting that these lysine residues are not critical for their functions. However, further studies are necessary for deep understanding of implication of these amino acid sequences.

HTLV-1 increases the number of infected cells by clonal proliferation of infected cells, which likely facilitates cell-to-cell transmission of this virus. Clonal proliferation of STLV-1-infected cells in Celebes macaques was demonstrated by the conventional inverse PCR method [15]. However, this technique could detect only a limited population of the clones because of its limited sensitivity or the stochastic amplification of the integration sites. In the present study, we investigated more comprehensively the clonal proliferation of infected cells in Japanese macaques naturally infected with STLV-1 by massively sequencing the unique integration sites of the provirus. The finding that STLV-1-infected cells proliferated clonally in the monkeys with higher proviral loads resembles the finding for HTLV-1. Furthermore, one monkey had lymphoma in the brain, showing that STLV-1 induces lymphoma in Japanese macaques. Analyses of STLV-1 integration sites in this T-cell lymphoma showed that one of the major clones in the brain was unique to this tumor, suggesting that this clone played an important role in the lymphomagenesis of this tumor.

This study also revealed a remarkable difference in STLV-1 seroprevalence between Japanese macaques (320/533: 60%) and rhesus macaques (1/163: 0.6%). Previous studies showed that the seroprevalence in rhesus macaques was 25%, and that in Japanese macaques was quite high [40-42]. Similarly, high seroprevalence was reported in baboons [43]. Furthermore, many studies reported the development of lymphoma in baboons [17,44,45]. The high seroprevalence and the development of lymphomas in Japanese macaques and baboons may suggest a higher susceptibility of these species to STLV-1 infection. Japanese macaques and baboons infected with STLV-1 may be suitable models for HTLV-1 research.

In this study, we also demonstrated that mogamulizumab strongly suppressed proviral load in STLV-1-infected Japanese macaques. Proviral load was suppressed for 4 weeks after the final administration of mogamulizumab, which seems reasonable when considering that the half-life of the

antibody administered at 1.0 mg/kg is approximately 18 days as measured in a clinical trial [46]. Some STLV-1-infected major clones recovered after the treatment, while other clones were still suppressed or even not detected. In HTLV-1-infected individuals, HTLV-1 proviral load is relatively constant in the chronic phase, although some minor clones fluctuate [25]. This study is the first to report that most of the major clones recover after the withdrawal of mogamulizumab. This observation suggests that the major clones may have some growth advantages that allow them to proliferate robustly *in vivo*. These growth advantages may be due to the integration site of the provirus, accumulation of genetic mutations, or epigenetic changes. The population of some clones remained constant over the course of the treatment. We speculate that these clones are negative for CCR4 expression. High proviral load is associated with risk of ATL and inflammatory diseases. Therefore, suppression of proviral load by mogamulizumab is a possible treatment for HTLV-1-associated inflammatory diseases such as HAM/TSP.

Conclusions

In summary, this study is the first to show that STLV-1 Tax and SBZ have activities similar to those of Tax and HBZ, activities which likely induce clonal proliferation and T-cell lymphoma in infected monkeys. STLV-1-infected Japanese macaques appear to be a good model for studying the effects of anti-viral drugs and the immunological aspects of HTLV-1 infection.

Methods

Biological samples of macaques

Japanese macaques (*Macaca fuscata*) and rhesus macaques (*Macaca mulatta*) used in this study were reared in the Primate Research Institute, Kyoto University. Blood samples were obtained from the macaques (for routine veterinary and microbiological examination) under ketamine anesthesia. All animal studies were conducted in accordance with the protocols of experimental procedures that were approved (2011–095) by the Animal Welfare and Animal Care Committee of the Primate Research Institute of Kyoto University, Inuyama, Japan.

Antibody screening and measurement of proviral load

Plasma samples were screened for the presence of antibodies against HTLV-1 by particle-agglutination test using SERODIA-HTLV-1 (Fujirebio). Proviral load was measured by real-time PCR quantifying the copy number of *tax* and *RAG1* as previously described [47]. Primers and probes are available in Additional file 4.

Detection of STLV-1 transcripts

Total RNA was extracted from STLV-1-infected Japanese macaque cell line Si-2 [48] with Trizol (Invitrogen), then cDNA was synthesized with SuperScript III (Invitrogen) using oligo dT primer. STLV-1 *tax* and *SBZ* was detected by PCR using primers (see Additional file 4) from the synthesized Si-2 cDNA: for STLV-1 *tax*, 2 min at 95°C, followed by 35 cycles of 20 seconds at 95°C, 10 seconds at 61°C, and 30 seconds at 72°C, and additional 5 min at 72°C; for SBZ, 2 min at 95°C, followed by 35 cycles of 20 seconds at 95°C, 10 seconds at 58°C, and 30 seconds at 72°C, and additional 5 min at 72°C. For comparison, HTLV-1 *tax* and *HBZ* were also amplified by PCR using cDNA of HTLV-1-infected cell lines (MT-1 or MT-2) with the same conditions. The primers used are shown in Additional file 4.

Plasmids

The PathDetect pNFκB-Luc, pAP-1-Luc and pNFAT-Luc plasmids were purchased from Stratagene. The 3TP-Lux, TopFlash reporter plasmids and WT-Luc were described previously [22,49]. The coding sequences of STLV-1 Tax and SBZ were amplified from STLV-1 provirus using oligos (see Additional file 4) and cloned into pME18Sneo to generate expression plasmids of STLV-1 Tax and SBZ. HTLV-1 tax was amplified using flanking primers (see Additional file 4) from pCGTax [50] and subcloned into pME18Sneo. The expression vector of HBZ cloned into pME18Sneo was described previously [11]. For the reporter assay, Jurkat cells or HepG2 cells were co-transfected with the reporter plasmid and the viral protein expression plasmids specified in each experiment, as previously described [22,24,51]. The activity of firefly luciferase was represented by normalizing to that of Renilla luciferase.

Retroviral vectors

The SBZ coding fragment was inserted into pGCDNSamI/N utilizing the NotI and SalI sites and SBZ-expressing retroviral vector was prepared as described previously [22].

Transduction of primary T-cells with retroviral vectors

$CD4^+CD25^-$ mouse T lymphocytes were stimulated and transduced with SBZ-expressing retroviral vector as previously described [22]. Forty-eight hours after the transduction, cells were harvested and analyzed by flow cytometry.

Flow cytometry

Antibodies used in this study were as follows: anti-human CD4 (OKT4), anti-Tax MI-73 [52], anti-mouse CD4 (RM4-5), anti-human CD271 (NGFR) (C40-1457), anti-mouse Foxp3 (FJK-16s), anti-human CD3 (SP34-2) and anti-human CCR4 (1G1, which recognizes a different epitope from that recognized by mogamulizumab). Intracellular staining was performed as previously described for Tax [52] and Foxp3 [22]. Cells were analyzed

by BD FACSCanto II with FACS Diva Software (BD Biosciences) or BD FACSVerse with FACSuite software (BD Biosciences).

Deep sequencing of provirus integration sites

The provirus integration sites in the Japanese macaque genome were amplified by linker-mediated PCR as previously described [27], with some modifications. Japanese macaque PBMC genomic DNA (3 μg) was sheared by sonication with a Bioruptor UCD-200 TM to obtain DNA fragments of approximately 200–500 bp. The ends of the DNA fragments were repaired to generate blunt ends using 18 units of T4 DNA polymerase, 5.3 units of DNA Klenow Polymerase I and 18 units of T4 polynucleotide kinase (TOYOBO) in T4 DNA ligase buffer (NEB) supplemented with 300 μM each of dNTP (TAKARA Bio). Adenine nucleotides were added to the blunt ends, and then linkers were ligated using 24 units of T4 DNA ligase (TOYOBO) in T4 DNA ligase buffer (NEB) utilizing the overhang of one thymidine nucleotide at the 3' end of the linker. The linker was generated by annealing two oligonucleotides (see Additional file 4). The first round of PCR was performed with the primers, STLV-1 Bio5 and Bio4. STLV-1 Bio5 anneals to the sequence within LTR of the STLV-1 provirus and Bio4 is the sequence present in the linker (see Additional file 4). Then, nested PCR was performed with the primers, Ion A-Bio7 and P1. In Ion A-Bio7, uppercase letters denote the sequence that anneals to the viral LTR downstream of STLV-1 Bio5, whereas the sequence in lowercase letters represents a tag specific for the Ion Torrent Personal Genome Machine (Ion PGM). P1 is also a tag specific for Ion PGM, which appears in the linker sequence (see Additional file 4). The amplification conditions of both the first and second PCR were 96°C for 30 sec, 7 cycles of 94°C for 5 sec and 72°C for 1 min, 23 cycles of 94°C for 5 sec and 68°C for 1 min, followed by additional 68°C for 9 min. Amplified fragments of approximately 150–300 bp were size-selected with E-Gel SizeSelect Agarose Gel (Life Technologies) and used as a DNA library in subsequent deep sequencing. Template beads to be sequenced with Ion Torrent Personal Genome Machine (Ion PGM) were prepared with the DNA library using the Ion PGM 200 Xpress Template Kit (Applied Biosystems) and subjected to sequencing on Ion Torrent 314 or 316 semiconductor chip using Ion PGM 200 Sequencing Kit (Applied Biosystems).

Deep sequencing data analysis

The host genomic sequences, located between the region immediately adjacent to the viral 3' LTR (ACACA) and the linker sequence (AGATCG), were extracted from the reads. Reads that started with GTTGGG (viral 5' LTR) were removed. Remaining reads were mapped to the reference genome of *Macaca mulatta* (MMUL 1.0) using the Burrows-Wheeler Aligner (BWA) [53]. Reads that were mapped only to single sites were analyzed. In order to obtain the absolute frequency of each provirus clone (the number of sister cells of the clone), the end position of each mapped read was obtained from the start position and cigar code in the SAM file generated by BWA. The reads with an identical start position and end position (integration site and shear site) were judged to derive from a single DNA fragment amplified by PCR, while reads with identical integration sites but distinct shear sites were judged to derive from different cells in a clone. In other words, the number of reads in the second category reflects the absolute frequency of each clone. Relative frequency represents the proportion of the absolute frequency of a clone to the number of all the sister cells observed. In order to minimize the distortion of relative frequencies of major clones, 6,000 reads that were mapped only to single sites were randomly selected for each specimen and analyzed (see Additional file 2).

Treatment of STLV-1$^+$ Japanese macaques with humanized anti-CCR4 antibody

Two Japanese macaques infected with STLV-1 were treated with mogamulizumab, which is an antibody against CCR4 and is approved in Japan as a drug to treat relapsed ATL. Mogamulizumab was provided by Kyowa Hakko Kirin Co Ltd. One mg/kg mogamulizumab was diluted in 40 ml saline and infused into each monkey intravenously for 20 min. Administration was performed once a week for 4 times. Before each administration, a 10 ml of blood sample was obtained. After the fourth administration, blood samples were collected every 2 weeks until week 11. Extra samples were collected on week 15 and week 18. The two monkeys were observed for any adverse effects during the experiment.

Additional files

Additional file 1: Phylogenetic analyses of HTLV-1 subtypes and Japanese macaque STLV-1.

Additional file 2: Deep sequencing data analysis.

Additional file 3: In vitro staining of Japanese macaque PBMCs with mogamulizumab.

Additional file 4: Primers and oligonucleotides.

Competing interests

Kyowa Hakko Kirin provided us the monoclonal antibody (mogamulizumab) that was used in this study.

Authors' contributions

JY and M. Matsuoka conceived of this study. JT carried out antibody screening and proviral load measurement. M. Miura, KS, GM and TZ carried out the molecular experiments and the reporter assays. AK, AW, AS and HA coordinated the macaque experiments and collected the macaque specimens. PM analyzed viral protein and surface marker expression. KO carried out immunohistochemistry and pathological analyses. M. Miura carried out massive sequencing and its data analysis. M. Miura, JY and M.

Matsuoka prepared the manuscript. All the authors approved the final manuscript.

Acknowledgements
We thank Masakazu Shimizu for technical support on massive sequencing with Ion Torrent PGM, Mayumi Morimoto and Yoshiro Kamanaka for technical assistance on monkey experiments, Linda Kingsbury for proof-reading, and Charles Bangham, and Heather Niederer for valuable advice on analyses of integration sites. This study was supported by a Grant-in-aid for Scientific Research from the Ministry of Education, Science, Sports, and Culture of Japan (221S0001), a grant from SENSHIN medical research foundation, a grant from Japan Leukaemia Research Fund to MM, and the Cooperation Research Program of the Primate Research Institute, Kyoto University.

Author details
[1]Laboratory of Virus Control, Institute for Virus Research, Kyoto University, Shogoin Kawahara-cho 53, Sakyo-ku, Kyoto 606-8507, Japan. [2]Department of Pathology, School of Medicine, Kurume University, Kurume, Fukuoka, Japan. [3]Center for Human Evolution Modeling Research, Primate Research Institute, Kyoto University, Inuyama, Aichi, Japan. [4]Present address: College of Chemistry and Life Sciences, Zhejiang Normal University, Jinhua, China.

Received: 18 August 2013 Accepted: 15 October 2013
Published: 24 October 2013

References

1. Gallo RC: **The discovery of the first human retrovirus: HTLV-1 and HTLV-2.** *Retrovirology* 2005, **2**:17.
2. Takatsuki K: **Discovery of adult T-cell leukemia.** *Retrovirology* 2005, **2**:16.
3. Gessain A, Cassar O: **Epidemiological aspects and world distribution of HTLV-1 infection.** *Front Microbiol* 2012, **3**:388.
4. Matsuoka M, Jeang KT: **Human T-cell leukaemia virus type 1 (HTLV-1) infectivity and cellular transformation.** *Nat Rev Cancer* 2007, **7**:270–280.
5. Gessain A, Boeri E, Yanagihara R, Gallo RC, Franchini G: **Complete nucleotide sequence of a highly divergent human T-cell leukemia (lymphotropic) virus type I (HTLV-I) variant from melanesia: genetic and phylogenetic relationship to HTLV-I strains from other geographical regions.** *Front Microbiol* 1993, **67**:1015–1023.
6. Osame M, Usuku K, Izumo S, *et al*: **HTLV-I associated myelopathy, a new clinical entity.** *Lancet* 1986, **1**:1031–1032.
7. Mochizuki M, Yamaguchi K, Takatsuki K, Watanabe T, Mori S, Tajima K: **HTLV-I and uveitis.** *Lancet* 1992, **339**:1110.
8. Bangham CR: **CTL quality and the control of human retroviral infections.** *Eur J Immunol* 2009, **39**:1700–1712.
9. Kawano N, Shimoda K, Ishikawa F, *et al*: **Adult T-cell leukemia development from a human T-cell leukemia virus type I carrier after a living-donor liver transplantation.** *Transplantation* 2006, **82**:840–843.
10. Tamaki H, Matsuoka M: **Donor-derived T-cell leukemia after bone marrow transplantation.** *N Engl J Med* 2006, **354**:1758–1759.
11. Satou Y, Yasunaga J, Yoshida M, Matsuoka M: **HTLV-I basic leucine zipper factor gene mRNA supports proliferation of adult T cell leukemia cells.** *Proc Natl Acad Sci U S A* 2006, **103**:720–725.
12. Hanon E, Hall S, Taylor GP, *et al*: **Abundant tax protein expression in CD4+ T cells infected with human T-cell lymphotropic virus type I (HTLV-I) is prevented by cytotoxic T lymphocytes.** *Blood* 2000, **95**:1386–1392.
13. Macnamara A, Rowan A, Hilburn S, *et al*: **HLA class I binding of HBZ determines outcome in HTLV-1 infection.** *PLoS Pathog* 2010, **6**:e1001117.
14. Watanabe T, Seiki M, Tsujimoto H, Miyoshi I, Hayami M, Yoshida M: **Sequence homology of the simian retrovirus genome with human T-cell leukemia virus type I.** *Virology* 1985, **144**:59–65.
15. Gabet AS, Gessain A, Wattel E: **High simian T-cell leukemia virus type 1 proviral loads combined with genetic stability as a result of cell-associated provirus replication in naturally infected, asymptomatic monkeys.** *Int J Cancer* 2003, **107**:74–83.
16. Tsujimoto H, Noda Y, Ishikawa K, *et al*: **Development of adult T-cell leukemia-like disease in African green monkey associated with clonal integration of simian T-cell leukemia virus type I.** *Cancer Res* 1987, **47**:269–274.
17. Voevodin A, Samilchuk E, Schatzl H, Boeri E, Franchini G: **Interspecies transmission of macaque simian T-cell leukemia/lymphoma virus type 1 in baboons resulted in an outbreak of malignant lymphoma.** *J Virol* 1996, **70**:1633–1639.
18. Cavanagh MH, Landry S, Audet B, *et al*: **HTLV-I antisense transcripts initiating in the 3'LTR are alternatively spliced and polyadenylated.** *Retrovirology* 2006, **3**:15.
19. Sun SC, Yamaoka S: **Activation of NF-kappaB by HTLV-I and implications for cell transformation.** *Oncogene* 2005, **24**:5952–5964.
20. Hall WW, Fujii M: **Deregulation of cell-signaling pathways in HTLV-1 infection.** *Oncogene* 2005, **24**:5965–5975.
21. Matsuoka M: **HTLV-1 bZIP factor gene: its roles in HTLV-1 pathogenesis.** *Mol Aspects Med* 2010, **31**:359–366.
22. Zhao T, Satou Y, Sugata K, *et al*: **HTLV-1 bZIP factor enhances TGF-{beta} signaling through p300 coactivator.** *Blood* 2011, **118**:1865–1876.
23. Satou Y, Yasunaga J, Zhao T, *et al*: **HTLV-1 bZIP factor induces T-cell lymphoma and systemic inflammation in vivo.** *PLoS Pathog* 2011, **7**:e1001274.
24. Ma G, Yasunaga J, Fan J, Yanagawa S, Matsuoka M: **HTLV-1 bZIP factor dysregulates the Wnt pathways to support proliferation and migration of adult T-cell leukemia cells.** *Oncogene* 2013, **32**:4222–4230.
25. Etoh K, Tamiya S, Yamaguchi K, *et al*: **Persistent clonal proliferation of human T-lymphotropic virus type I-infected cells in vivo.** *Cancer res* 1997, **57**:4862–4867.
26. Wattel E, Vartanian JP, Pannetier C, Wain-Hobson S: **Clonal expansion of human T-cell leukemia virus type I-infected cells in asymptomatic and symptomatic carriers without malignancy.** *J Virol* 1995, **69**:2863–2868.
27. Gillet NA, Malani N, Melamed A, *et al*: **The host genomic environment of the provirus determines the abundance of HTLV-1-infected T-cell clones.** *Blood* 2011, **117**:3113–3122.
28. Yoshie O, Fujisawa R, Nakayama T, *et al*: **Frequent expression of CCR4 in adult T-cell leukemia and human T-cell leukemia virus type 1-transformed T cells.** *Blood* 2002, **99**:1505–1511.
29. Ishii T, Ishida T, Utsunomiya A, *et al*: **Defucosylated humanized anti-CCR4 monoclonal antibody KW-0761 as a novel immunotherapeutic agent for adult T-cell leukemia/lymphoma.** *Clin Cancer Res* 2010, **16**:1520–1531.
30. Yamano Y, Araya N, Sato T, *et al*: **Abnormally high levels of virus-infected IFN-gamma+ CCR4+ CD4+ CD25+ T cells in a retrovirus-associated neuroinflammatory disorder.** *PLoS One* 2009, **4**:e6517.
31. Souquiere S, Mouinga-Ondeme A, Makuwa M, *et al*: **T-cell tropism of simian T-cell leukaemia virus type 1 and cytokine profiles in relation to proviral load and immunological changes during chronic infection of naturally infected mandrills (Mandrillus sphinx).** *J Med Primatol* 2009, **38**:279–289.
32. Stevens HP, Holterman L, Haaksma AG, Jonker M, Heeney JL: **Lymphoproliferative disorders developing after transplantation and their relation to simian T-cell leukemia virus infection.** *Transpl Int* 1992, **5**(Suppl 1):S450–S453.
33. Akari H, Ono F, Sakakibara I, *et al*: **Simian T cell leukemia virus type I-induced malignant adult T cell leukemia-like disease in a naturally infected African green monkey: implication of CD8+ T cell leukemia.** *AIDS Res Hum Retroviruses* 1998, **14**:367–371.
34. McCarthy TJ, Kennedy JL, Blakeslee JR, Bennett BT: **Spontaneous malignant lymphoma and leukemia in a simian T-lymphotropic virus type I (STLV-I) antibody positive olive baboon.** *Lab Anim Sci* 1990, **40**:79–81.
35. Sakakibara I, Sugimoto Y, Sasagawa A, *et al*: **Spontaneous malignant lymphoma in an African green monkey naturally infected with simian T-lymphotropic virus (STLV).** *J Med Primatol* 1986, **15**:311–318.
36. Afonso PV, Mekaouche M, Mortreux F, *et al*: **Highly active antiretroviral treatment against STLV-1 infection combining reverse transcriptase and HDAC inhibitors.** *Blood* 2010, **116**:3802–3808.
37. Zhao T, Yasunaga J, Satou Y, *et al*: **Human T-cell leukemia virus type 1 bZIP factor selectively suppresses the classical pathway of NF-kappaB.** *Blood* 2009, **113**:2755–2764.
38. Basbous J, Arpin C, Gaudray G, Piechaczyk M, Devaux C, Mesnard JM: **The HBZ factor of human T-cell leukemia virus type I dimerizes with transcription factors JunB and c-Jun and modulates their transcriptional activity.** *J Biol Chem* 2003, **278**:43620–43627.
39. Clerc I, Polakowski N, Andre-Arpin C, *et al*: **An interaction between the human T cell leukemia virus type 1 basic leucine zipper factor (HBZ) and the KIX domain of p300/CBP contributes to the down-regulation of tax-dependent viral transcription by HBZ.** *J Biol Chem* 2008, **283**:23903–23913.
40. Lairmore MD, Lerche NW, Schultz KT, *et al*: **SIV, STLV-I and type D retrovirus antibodies in captive rhesus macaques and immunoblot**

reactivity to SIV p27 in human and rhesus monkey sera. *AIDS Res Hum Retroviruses* 1990, **6**:1233–1238.
41. Miyoshi I, Fujishita M, Taguchi H, Matsubayashi K, Miwa N, Tanioka Y: **Natural infection in non-human primates with adult T-cell leukemia virus or a closely related agent.** *Int J Cancer* 1983, **32**:333–336.
42. Miyoshi I, Yoshimoto S, Fujishita M, *et al*: **Natural adult T-cell leukemia virus infection in Japanese monkeys.** *Lancet* 1982, **2**:658.
43. Takemura T, Yamashita M, Shimada MK, *et al*: **High prevalence of simian T-lymphotropic virus type L in wild ethiopian baboons.** *J Virol* 2002, **76**:1642–1648.
44. Graves LE, Hennessy A, Sunderland NS, Heffernan SJ, Thomson SE: **Incidence of lymphoma in a captive-bred colony of hamadryas baboons (Papio hamadryas).** *Aust Vet J* 2009, **87**:238–243.
45. Hubbard GB, Mone JP, Allan JS, *et al*: **Spontaneously generated non-Hodgkin's lymphoma in twenty-seven simian T-cell leukemia virus type 1 antibody-positive baboons (Papio species).** *Lab Anim Sci* 1993, **43**:301–309.
46. Yamamoto K, Utsunomiya A, Tobinai K, *et al*: **Phase I study of KW-0761, a defucosylated humanized anti-CCR4 antibody, in relapsed patients with adult T-cell leukemia-lymphoma and peripheral T-cell lymphoma.** *J Clin Oncol* 2010, **28**:1591–1598.
47. Yasunaga J, Sakai T, Nosaka K, *et al*: **Impaired production of naive T lymphocytes in human T-cell leukemia virus type I-infected individuals: its implications in the immunodeficient state.** *Blood* 2001, **97**:3177–3183.
48. Miyoshi I, Yoshimoto S, Fujishita M, *et al*: **Isolation in culture of a type C virus from a Japanese monkey seropositive to adult T-cell leukemia-associated antigens.** *Gann* 1983, **74**:323–326.
49. Yanagawa S, Lee JS, Matsuda Y, Ishimoto A: **Biochemical characterization of the Drosophila axin protein.** *FEBS Lett* 2000, **474**:189–194.
50. Fujisawa J, Toita M, Yoshimura T, Yoshida M: **The indirect association of human T-cell leukemia virus tax protein with DNA results in transcriptional activation.** *J Virol* 1991, **65**:4525–4528.
51. Sugata K, Satou Y, Yasunaga J, *et al*: **HTLV-1 bZIP factor impairs cell-mediated immunity by suppressing production of Th1 cytokines.** *Blood* 2012, **119**:434–444.
52. Satou Y, Utsunomiya A, Tanabe J, Nakagawa M, Nosaka K, Matsuoka M: **HTLV-1 modulates the frequency and phenotype of FoxP3+CD4+ T cells in virus-infected individuals.** *Retrovirology* 2012, **9**:46.
53. Li H, Durbin R: **Fast and accurate short read alignment with Burrows-Wheeler transform.** *Bioinformatics* 2009, **25**:1754–1760.

doi:10.1186/1742-4690-10-118
Cite this article as: Miura *et al.*: Characterization of simian T-cell leukemia virus type 1 in naturally infected Japanese macaques as a model of HTLV-1 infection. *Retrovirology* 2013 **10**:118.

HTLV-1 bZIP Factor Induces Inflammation through Labile Foxp3 Expression

Nanae Yamamoto-Taguchi[1], Yorifumi Satou[1], Paola Miyazato[1], Koichi Ohshima[2], Masanori Nakagawa[3], Koko Katagiri[4], Tatsuo Kinashi[5], Masao Matsuoka[1]*

1 Laboratory of Virus Control, Institute for Virus Research, Kyoto University, Kyoto, Japan, **2** Department of Pathology, School of Medicine, Kurume University, Fukuoka, Japan, **3** Department of Neurology, Graduate School of Medical Science, Kyoto Prefectural University of Medicine, Kyoto, Japan, **4** Department of Biosciences, School of Science, Kitasato University, Kanagawa, Japan, **5** Department of Molecular Genetics, Institute of Biomedical Science, Kansai Medical University, Osaka, Japan

Abstract

Human T-cell leukemia virus type 1 (HTLV-1) causes both a neoplastic disease and inflammatory diseases, including HTLV-1-associated myelopathy/tropical spastic paraparesis (HAM/TSP). The HTLV-1 basic leucine zipper factor (HBZ) gene is encoded in the minus strand of the proviral DNA and is constitutively expressed in infected cells and ATL cells. HBZ increases the number of regulatory T (Treg) cells by inducing the *Foxp3* gene transcription. Recent studies have revealed that some $CD4^+Foxp3^+$ T cells are not terminally differentiated but have a plasticity to convert to other T-cell subsets. Induced Treg (iTreg) cells tend to lose Foxp3 expression, and may acquire an effector phenotype accompanied by the production of inflammatory cytokines, such as interferon-γ (IFN-γ). In this study, we analyzed a pathogenic mechanism of chronic inflammation related with HTLV-1 infection via focusing on HBZ and Foxp3. Infiltration of lymphocytes was observed in the skin, lung and intestine of HBZ-Tg mice. As mechanisms, adhesion and migration of HBZ-expressing $CD4^+$ T cells were enhanced in these mice. $Foxp3^-CD4^+$ T cells produced higher amounts of IFN-γ compared to those from non-Tg mice. Expression of Helios was reduced in Treg cells from HBZ-Tg mice and HAM/TSP patients, indicating that iTreg cells are predominant. Consistent with this finding, the conserved non-coding sequence 2 region of the *Foxp3* gene was hypermethylated in Treg cells of HBZ-Tg mice, which is a characteristic of iTreg cells. Furthermore, Treg cells in the spleen of HBZ-transgenic mice tended to lose Foxp3 expression and produced an excessive amount of IFN-γ, while Foxp3 expression was stable in natural Treg cells of the thymus. HBZ enhances the generation of iTreg cells, which likely convert to $Foxp3^-$T cells producing IFN-γ. The HBZ-mediated proinflammatory phenotype of $CD4^+$ T cells is implicated in the pathogenesis of HTLV-1-associated inflammation.

Citation: Yamamoto-Taguchi N, Satou Y, Miyazato P, Ohshima K, Nakagawa M, et al. (2013) HTLV-1 bZIP Factor Induces Inflammation through Labile Foxp3 Expression. PLoS Pathog 9(9): e1003630. doi:10.1371/journal.ppat.1003630

Editor: Jeremy Luban, University of Massachusetts Medical School, United States of America

Received April 11, 2013; **Accepted** August 1, 2013; **Published** September 19, 2013

Funding: This study was supported by a Grant-in-Aid for Scientific Research from the Ministry of Education, Science, Sports, and Culture of Japan (22114003), and a grant from SENSHIN medical research foundation, and a grant from Japan Leukaemia Research Fund to MM; a grant from Takeda Science Foundation; and a grant from Naito Foundation to YS. The funders had no role in study design, data collection and analysis, decision to publish, or preparation of the manuscript.

Competing Interests: The authors have declared that no competing interests exist.

* E-mail: mmatsuok@virus.kyoto-u.ac.jp

Introduction

Human T-cell leukemia virus type 1 (HTLV-1) is known to be the causal agent of a neoplastic disease of $CD4^+$ T cells, adult T-cell leukemia (ATL) [1]. In addition, this virus perturbs the host immune system, causing inflammatory diseases and immunodeficiency. Inflammatory diseases associated with HTLV-1 include HTLV-1-associated myelopathy/tropical spastic paraparesis (HAM/TSP) [2,3], uveitis [4,5], alveolitis [6], infective dermatitis [7] and myositis [8]. Increased expression of inflammatory cytokines and immune response to the Tax antigen has been proposed as mechanisms of these inflammatory diseases [9]. However, the detailed mechanisms of inflammation remain elusive.

The *HTLV-1 bZIP factor* (*HBZ*) gene is encoded in the minus strand of the provirus and consistently expressed in ATL cases and HTLV-1-infected individuals [10]. *In vitro* and *in vivo* experiments have shown that the *HBZ* gene promotes the proliferation of T cells and increases their number [10,11]. Recently, we reported that HBZ transgenic (HBZ-Tg) mice develop both T-cell lymphomas and inflammatory diseases [12]. In HBZ-Tg mice, we found that the number of $CD4^+$ T cells expressing Foxp3, a master molecule for regulatory T (Treg) cells, was remarkably increased. HBZ induces transcription of the *Foxp3* gene via interaction with Smad2/3 and a co-activator, p300, resulting in an increased number of $Foxp3^+$ T cells [13]. Concurrently, HBZ interacts with Foxp3 and decreases the immune suppressive function [12]. This interaction could be a mechanism of the inflammatory phenotype observed in HBZ-Tg mice. However, detailed mechanisms to induce inflammation by HBZ remain unsolved.

Treg cells suppress excessive immune responses, and control the homeostasis of the immune system [14]. Foxp3 is considered a marker of Treg cells, yet several lines of evidence have shown that there is heterogeneity within $Foxp3^+$cells [15]. Natural Treg (nTreg) cells are generated in the thymus while induced Treg (iTreg) cells are induced in the peripheral lymphoid organs. It has been reported that Treg cells that have lostFoxp3 expression (exFoxp3 T cells) produce interferon-γ (IFN-γ), indicating that$Foxp3^+$ Treg cells are not terminally differentiated cells but

Author Summary

Viral infection frequently induces tissue inflammation in the host. HTLV-1 infection is associated with chronic inflammation in the CNS, skin, and lung, but the inflammatory mechanism is not fully understood yet. Since HTLV-1 directly infects $CD4^+$ T cells, central player of the host immune regulation, HTLV-1 should modulate the host immune response not only via viral antigen stimulation but also via $CD4^+$ T-cell-mediated immune deregulation. It has been reported that $Foxp3^+CD4^+$ T cells are increased in HTLV-1 infection. It remains a central question in HTLV-1 pathogenesis why HTLV-1 induces inflammation despite of increase of $FoxP3^+$ cells, which generally possess immune suppressive function. We have elucidated here that most of the increased $Foxp3^+$ cells in HBZ-Tg mice or HAM/TSP patients is not thymus-derived naturally occurring Treg cells but induced Treg cells. Since the iTreg cells are prone to lose FoxP3 expression and then become cytokine-producing cells, the increase of iTreg cells could serve as a source of proinflammatory $CD4^+$ T cells. Thus HTLV-1 causes abnormal $CD4^+$ T-cell differentiation by expressing HBZ, which should play a crucial role in chronic inflammation related with HTLV-1. This study has provided new insights into the mechanism of chronic inflammation accompanied with viral infection.

susceptible to conversion into effector T cells according to their environment [16]. Recently, Miyao et al. have reported that $Foxp3^+$ T cells induced by activation exhibit transient Foxp3 expression, and become exFoxp3 T cells [17]. Even though the plasticity of Treg cells remains controversial [18], these reports suggest that $Foxp3^+$ T cells possess not only suppressive function but also proinflammatory attributes.

In this study, we found that iTreg cells increased in HBZ-Tg mice and that Treg cells of HBZ-Tg mice tend to lose Foxp3 expression, leading to increased IFN-γ-expressing proinflammatory cells. Cell adhesion and migration are enhanced in $CD4^+$ T cells of HBZ-Tg mice. Thus, these HBZ-mediated abnormalities of CD4 T cells play critical roles in inflammatory diseases caused by HTLV-1.

Results

HBZ-Tg mice spontaneously develop inflammation

We have reported that HBZ-Tg mice develop both T-cell lymphoma and inflammatory diseases including dermatitis and alveolitis [12]. To further study the inflammatory changes affecting HBZ-Tg mice, we analyzed various tissues and organs in detail. In HBZ-Tg mice, moderate lymphoid cell infiltration was detected in the peri-bronchial space of the lung (Figure 1A), the peri-follicular area of the skin (Figure 1B), the mucosa of the small intestine (Figure 1C), and the mucosa of the colon (Figure 1D). Meanwhile, there was no obvious evidence of inflammation in liver, kidney or spinal cord. In non-Tg littermates, infiltration of lymphoid cells was not observed in skin, lung or intestine. These findings suggest the inflammatory involvement of multiple tissues and organs in HBZ-Tg mice.

Enhanced cell adhesion and migration of HBZ-Tg $CD4^+$ T cells

Infiltration of lymphocytes into various tissues suggests that the lymphocytes of HBZ-Tg mice have increased adhesive ability. We first studied the expression of LFA-1, which is a heterodimer of CD11a and CD18. As shown in Figure 2A, both CD11a and

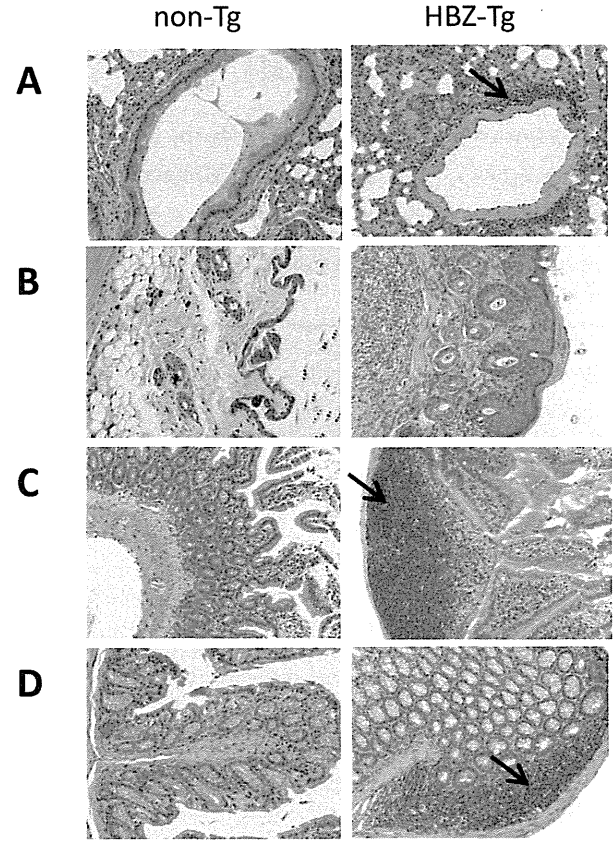

Figure 1. Histopathology of mouse inflammatory tissue. Hematoxylin and eosin staining of lung (A), skin (B), small intestine (C) and large intestine (D) from non-Tg littermate mice (left) or HBZ-Tg mice (right). Original magnification, ×10. Arrows indicate massive infiltration of lymphocytes.
doi:10.1371/journal.ppat.1003630.g001

CD18 were upregulated on HBZ-Tg $CD4^+$ T cells of spleen, lung and lymph nodes compared with $CD4^+$ T cells from non-Tg mice. In addition, the expression of CD103 (alpha E integrin) on HBZ-Tg $CD4^+$ T cells was also higher than that on non-Tg $CD4^+$ T cells. These findings suggest an increased adhesive capability of $CD4^+$ T cells in HBZ-Tg mice. Immunohistochemical analyses of lung and intestine of HBZ-Tg mice confirmed increased expression of these molecules, particularly CD18 (Figure 2B, C).

Expression of CD11a, CD18 and CD103 was also studied in HAM/TSP patients. In addition to healthy donors, we analyzed expression of these molecules on HTLV-1 infected cells that are identified using anti-Tax antibody. As shown in Figure 2D, CD11a and CD18 expression of $CD4^+Tax^+$ T cells was upregulated compared with $CD4^+$ T cells from healthy donors and $CD4^+Tax^-$ T cells of HAM/TSP patients while expression of CD103 was not different among these cells. These results show that enhanced expression of LFA-1 is also observed in HTLV-1 infected cells in HAM/TSP patients.

We next investigated adhesion of $CD4^+$ T cells to ICAM-1, since ICAM-1 is critical for lymphocyte migration and adhesion to vascular epithelial cells in an inflammatory lesion. We isolated $CD4^+$ T cells from non-Tg or HBZ-Tg splenocytes, placed them on ICAM-1-coated 96-well plates, and evaluated cell adhesion activity to ICAM-1. $CD4^+$ T cells from HBZ-Tg mice showed increased adhesion in the absence of stimulation, while no difference was found when cells were stimulated by anti-CD3 antibody (Figure 3A). Furthermore, we

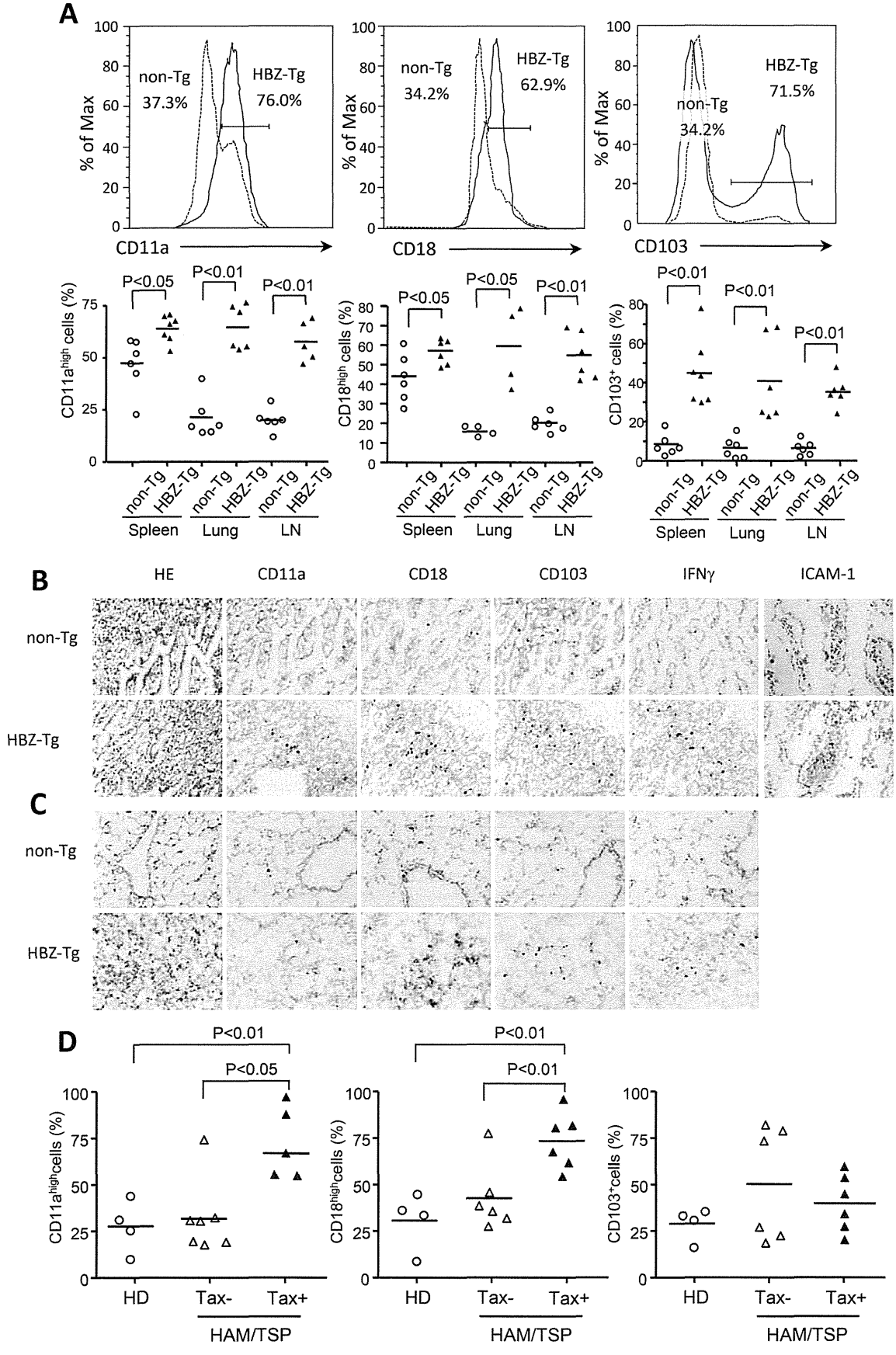
A
non-Tg
37.3%
HBZ-Tg
76.0%
% of Max
CD11a
non-Tg
34.2%
HBZ-Tg
62.9%
CD18
non-Tg
34.2%
HBZ-Tg
71.5%
CD103
CD11a^high cells (%)
CD18^high cells (%)
CD103+ cells (%)
P<0.05
P<0.01
non-Tg
HBZ-Tg
Spleen
Lung
LN
B
HE
CD11a
CD18
CD103
IFNγ
ICAM-1
non-Tg
HBZ-Tg
C
non-Tg
HBZ-Tg
D
P<0.01
P<0.05
CD11a^high cells (%)
CD18^high cells (%)
CD103+ cells (%)
HD
Tax-
Tax+
HAM/TSP

Figure 2. Expression of CD11a, CD18 and CD103 in CD4$^+$T cells from spleen, lung and LN cells isolated from HBZ-Tg mice. (A) The expression of CD11a, CD18 and CD103 in CD4$^+$ T cells from non-Tg (dashed line) and HBZ-Tg (solid line) mice was analyzed by flow cytometry. Histograms from one representative mouse splenocytes of each group are shown (top panels). The bottom panel shows the results of 4 or 6 mice in each group, each symbol representing an individual mouse. The small horizontal lines indicate the mean. Frozen sections of intestine (B) and lung (C) of non-Tg and HBZ-Tg mice were stained with HE and the indicated antibodies. Original magnification is ×20. Results from one representative mouse of each group are shown. (D) CD11a, CD18 and CD103 expressions are shown on CD4$^+$ cells from HDs, CD4$^+$Tax$^-$ and CD4$^+$Tax$^+$ cells from HAM/TSP patients.
doi:10.1371/journal.ppat.1003630.g002

evaluated the migration activity of CD4$^+$ T cells on ICAM-1-coated plates. To induce cell migration, we stimulated CD4$^+$ T cells with CCL22 as reported previously [19]. Cell migration of HBZ-Tg CD4$^+$ T cells was also increased compared with migration of non-Tg CD4$^+$ T cells (Figure 3B). These results demonstrate an infiltrative phenotype of CD4$^+$ T cells in HBZ-Tg mice.

Infiltration of LFA-1 expressing T cells into various tissues suggests that ICAM-1 expression is enhanced. Indeed, expression of ICAM-1 was increased in intestine of HBZ-Tg mice (Figure 2B). Enhanced migration of CD4$^+$ T cells suggests involvement of chemokine(s)-chemokine receptor for HBZ-Tg mice. We analyzed expression of chemokine receptors on CD4$^+$ T cells of HBZ-Tg mice. As shown in Figure 3C, CXCR3 expression of CD4$^+$ splenocytes was increased while expression of CCR5 and CCR7 were not different compared with control mice (Figure S1). CXCR3 expression of CD4$^+$ T cells was upregulated in both lung and lymph node (Figure 3C). Although the ligands for CXCR3, CXCL9 and CXCL10, were not increased in the sera of HBZ-Tg

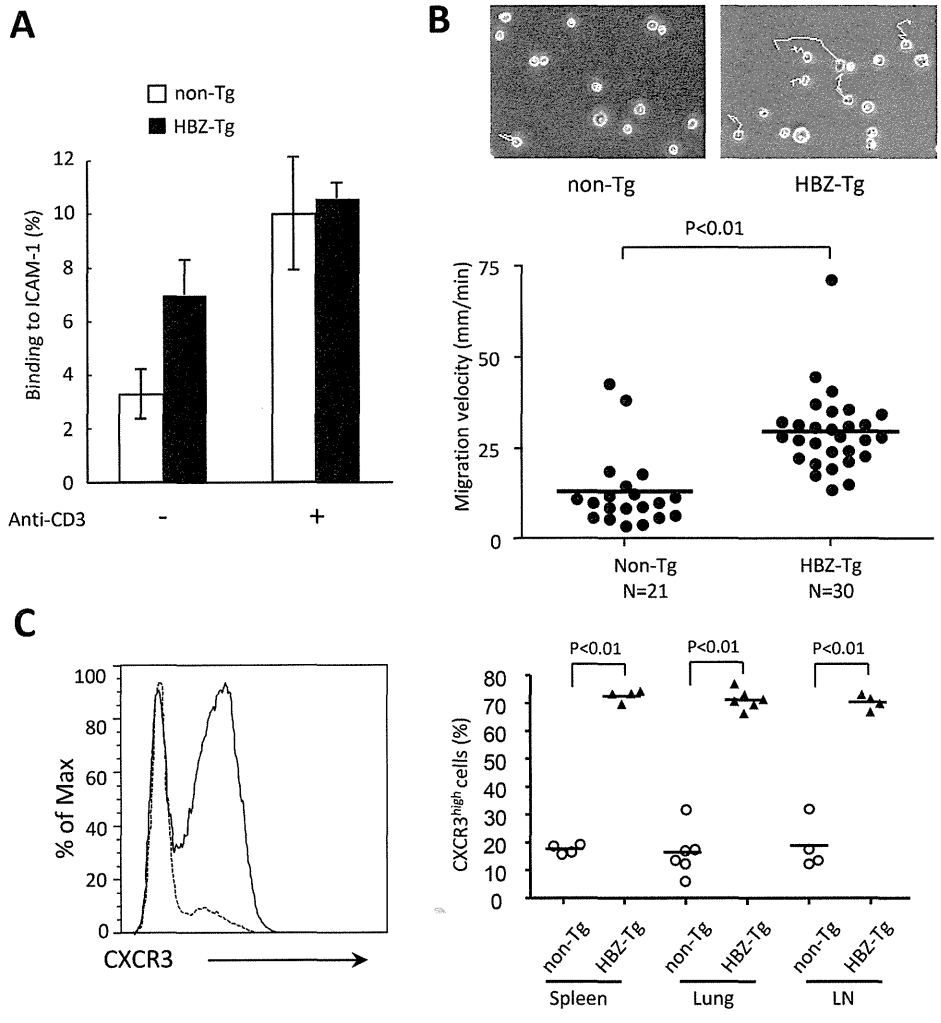

Figure 3. Enhanced capacity for cell adhesion and migration of CD4$^+$splenocytes isolated from HBZ-Tg mice. (A) Assays of cell adhesion to mouse ICAM-1 were performed using purified mouse CD4$^+$splenocytes of HBZ-Tg or non-Tg mice. Results shown are means ± s.d. of triplicate wells. (B) Random CD4$^+$ mouse splenocyte migration was recorded at 37°C with a culture dish system for live-cell microscopy. Phase-contrast images were taken every 15 seconds for 10 min. The cells were traced and migration velocity was calculated. Each dot represents the velocity of an individual cell, and bars indicate the mean (n = 21 for non-Tg, n = 30 for HBZ-Tg). Statistical analyses were performed using an unpaired, two-tailed Student *t*-test. (C) Representative histograms of CXCR3 expression in CD4$^+$ T cells from non-Tg (dashed line) and HBZ-Tg (solid line) mice (left) and cumulative results from 4 or 6 mice are shown in the graph (right) for spleen, lung and lymph node. Each symbol represents an individual mouse; small horizontal lines indicate the mean.
doi:10.1371/journal.ppat.1003630.g003

mice (Figure S1), CXCR3 might be implicated in infiltration of $CD4^+$ T cells.

Pro-inflammatory cytokine production by $CD4^+$ T cells in the HBZ-Tg mice

To elucidate the mechanism of the pro-inflammatory phenotype observed in HBZ-Tg mice, we investigated cytokine production in $CD4^+$ T cells of the spleen. After stimulation by PMA/ionomycin, production of IFN-γ was increased in $CD4^+$ T cells while that of TNF-α was suppressed (Figure 4A). There were no significant differences between HBZ-Tg mice and non-Tg mice in IL-2, IL-4 and IL-17 production by $CD4^+$ T cells. We have reported that the number of $Foxp3^+CD4^+$ Treg cells is increased in HBZ-Tg mice. Therefore, we simultaneously stained both intracellular cytokines and Foxp3 to distinguish the cytokine production of $CD4^+Foxp3^-$ T cells from that of $CD4^+Foxp3^+$ T cells. Production of TNF-α, IL-17 and IL-2 was slightly increased in $CD4^+Foxp3^+$ T cells of HBZ-Tg mice (Figure 4B, C). Since Foxp3 suppresses production of cytokines [19], and HBZ impairs function of Foxp3 [12], HBZ-mediated impairment of Foxp3 function might be a mechanism of this increased expression of these cytokines. However, TNF-α production was suppressed in $CD4^+$ $Foxp3^-$ T cells and total $CD4^+$ T cells (Figure 4A, C). In particular, IFN-γ production of splenic $CD4^+Foxp3^-$ T cells from HBZ-Tg mice was remarkably increased compared with those from non-Tg mice (Figure 4B). We also studied IFN-γ production in $CD4^+$ T cells of

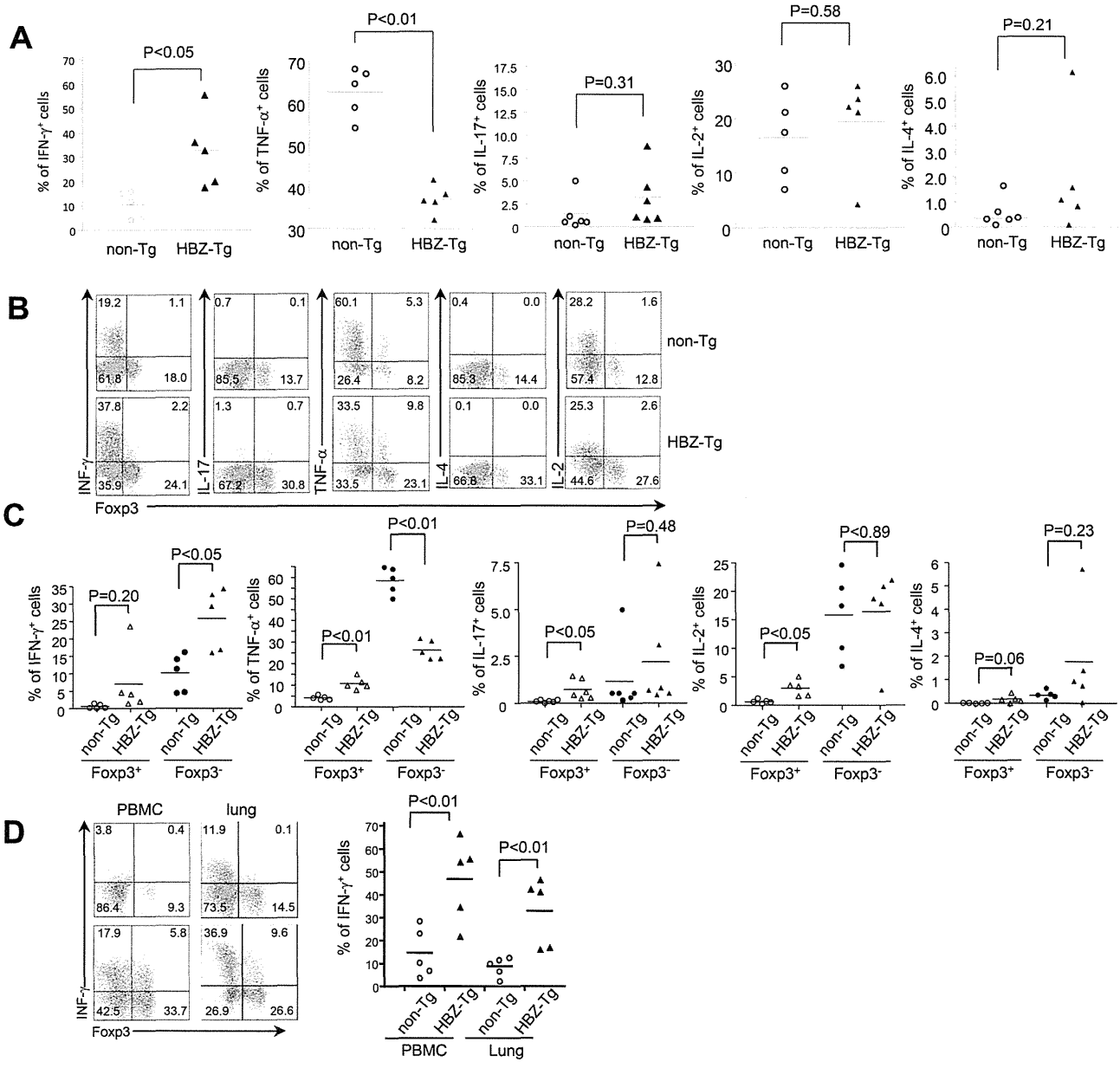

Figure 4. Production of cytokines in HBZ-Tg mice. (A) Splenocytes of HBZ-Tg mice or non-Tg mice were stimulated with PMA/ionomycin and protein transport inhibitor for 4 h. IFN-γ, IL-17, TNF-α, IL-4 or IL-2 production was analyzed in $CD4^+$ T cells by flow cytometry. (B) Cytokine production was analyzed along with Foxp3 expression. (C) Production of cytokines was shown in $CD4^+Foxp3^+$ T cells and $CD4^+Foxp3^-$ T cells. (D) IFN-γ and Foxp3 expression gated on $CD4^+$ T cells from PBMC or cells isolated from the lungs were analyzed by flow cytometry. Percentage of $IFN\text{-}\gamma^+$ cells in $CD4^+$ splenocytes, PBMC and lung cells. Each symbol represents an individual mouse; small horizontal lines indicate the mean.
doi:10.1371/journal.ppat.1003630.g004

PBMCs and lung-infiltrating lymphocytes. The production of IFN-γ was remarkably increased in PBMC and lung from HBZ-Tg mice (Figure 4D). Taken together, these results suggest that increased IFN-γ production, especially in $CD4^+Foxp3^-$ T cells, is related to the chronic inflammation observed in HBZ-Tg mice. Immunohistochemical analyses also showed that IFN-γ production was increased in both lung and intestine of HBZ-Tg mice (Figure 2B, C).

Increased number of induced Treg cells in HBZ-Tg mice

We have reported that HBZ enhances the transcription of the *Foxp3* gene in cooperation with TGF-ß, leading to an increased number of Treg cells *in vivo* [12,13]. Two types of Treg cells have been reported: natural Treg (nTreg) cells and induced Treg (iTreg) cells in $CD4^+Foxp3^+$ cells. The expression of Helios, a member of the Ikaros family of transcription factors, is considered a marker of nTreg cells [20]. To determine which Treg cell population is increased in HBZ-Tg mice, we analyzed the expression of Helios. Expression of Helios in $CD4^+Foxp3^+$ T cells in HBZ-Tg mice was lower than that in non-Tg mice (Figure 5A, C), suggesting that the number of iTreg cells is increased in HBZ-Tg mice. A higher proportion of $CD4^+Foxp3^+Helios^{low}$ cells were found in the lungs of HBZ-Tg mice (Figure S2). Next, we analyzed the expression of Helios in Treg cells from HAM/TSP patients. As shown in Figure 5 B and D, Helios expression of Treg cells in HAM/TSP patients was lower than that of Treg cells in healthy controls. We also analyzed Helios expression in $Foxp3^+$ T (nTreg) cells of the thymus. The level of Helios expression in nTreg cells in HBZ-Tg mice was equivalent to that of non-Tg mice (Figure S3). These data collectively suggest that the iTreg cell population is increased not only in HBZ-Tg mice, but also in HAM/TSP patients.

Recent studies have reported that Helios expression is not always associated with nTreg cells [21–23]. A previous study reported that conserved non-coding DNA sequence (CNS) elements in the *Foxp3* locus play an important role in the induction and maintenance of *Foxp3* gene expression [24]. Among these elements, CNS2, methylated in iTreg cells, was suggested to be responsible for the lack of stable expression of Foxp3 in these cells [24]. This region is not methylated in Helios- nTreg cells, indicating that unmethylation of this region is a suitable marker of nTreg cells [21]. Therefore, we sorted the Treg fraction from HBZ-Tg or non-Tg mice splenocytes, extracted genomic DNA, and determined the DNA methylation status in the CNS2 region of the *Foxp3* gene. The results revealed

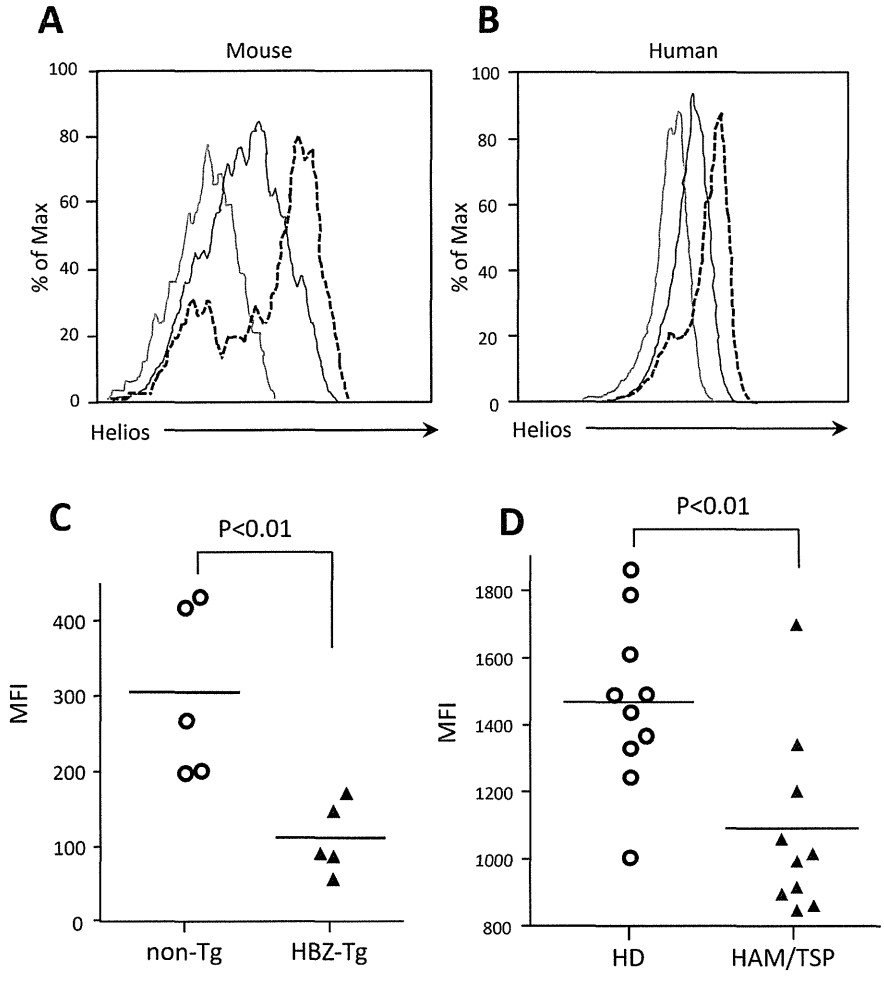

Figure 5. Helios expression in HBZ-Tg mice and HAM/TSP patients. (A) Expression of Helios in $CD4^+Foxp3^+$ cells of HBZ-Tg mice (solid line), non-Tg mice (dashed line) and isotype control (filled histogram). (B) Intracellular Helios expression in gated $CD4^+$ T cells from HAM/TSP patients (solid line), healthy donors (dashed line), or isotype control (filled histogram). One representative histogram for each group is shown. (C) Results from 5 non-Tg and 5 HBZ-Tg mice are shown. (D) Comparison of Helios expression in $CD4^+FoxP3^+$PBMC's from 10 HAM/TSP patients and 10 healthy donors. Each symbol represents the value for an individual subject. Statistical analyses were performed using an unpaired, two-tailed Student *t*-test.
doi:10.1371/journal.ppat.1003630.g005

that in HBZ-Tg $CD4^+Foxp3^+$ T cells, the CNS2 region had a higher methylation status than in non-Tg $CD4^+Foxp3^+$ cells (Figure 6), indicating that the increase in $CD4^+Foxp3^+$ cells in HBZ-Tg mice indeed mostly consists of iTreg cells.

Foxp3 expression in $CD4^+Foxp3^+$ T cells in HBZ-Tg mice is unstable, leading to the generation of exFoxp3 T cells expressing IFN-γ

Recent studies have revealed that $CD4^+Foxp3^+$ T cells are not terminally differentiated but have the plasticity to convert to other T cell subsets [25]. When Treg cells lose the expression of Foxp3 (exFoxp3 T cells), such cells produce pro-inflammatory cytokines [16]. It has been reported that Foxp3 expression in nTreg cells is stable but that it is not in iTreg cells [15]. These findings suggest that in HBZ-Tg mice, which have greater numbers of iTreg cells as shown in this study, Foxp3 expression in these cells tends to diminish, letting these cells acquire an effector phenotype associated with the production of pro-inflammatory cytokines such as IFN-γ. To investigate this possibility, we sorted Treg cells from the spleens of HBZ-Tg or non-Tg mice based on their expression of CD4, CD25 and GITR; cultured them for 7 days; and analyzed Foxp3 expression by flow cytometry. After 7 days in culture, the percentage of $Foxp3^+$ T cells diminished remarkably in HBZ-Tg mice compared with non-Tg mice (Figure 7A, B). We investigated the production of IFN-γ at this point, and found that it was increased in $Foxp3^-$ T cells from HBZ-Tg mice compared with those from non-Tg mice (Figure 7C). In sharp contrast to this finding, Foxp3 expression of nTreg cells did not change in $CD4^+$ thymocytes of HBZ-Tg mice (Figure 7D). Collectively, these data indicate thatFoxp3 expression in nTreg cells is stable in HBZ-Tg mice, while most of the Treg cells in the periphery are iTreg cells. The enhanced generation of exFoxp3 T cells in the periphery is a

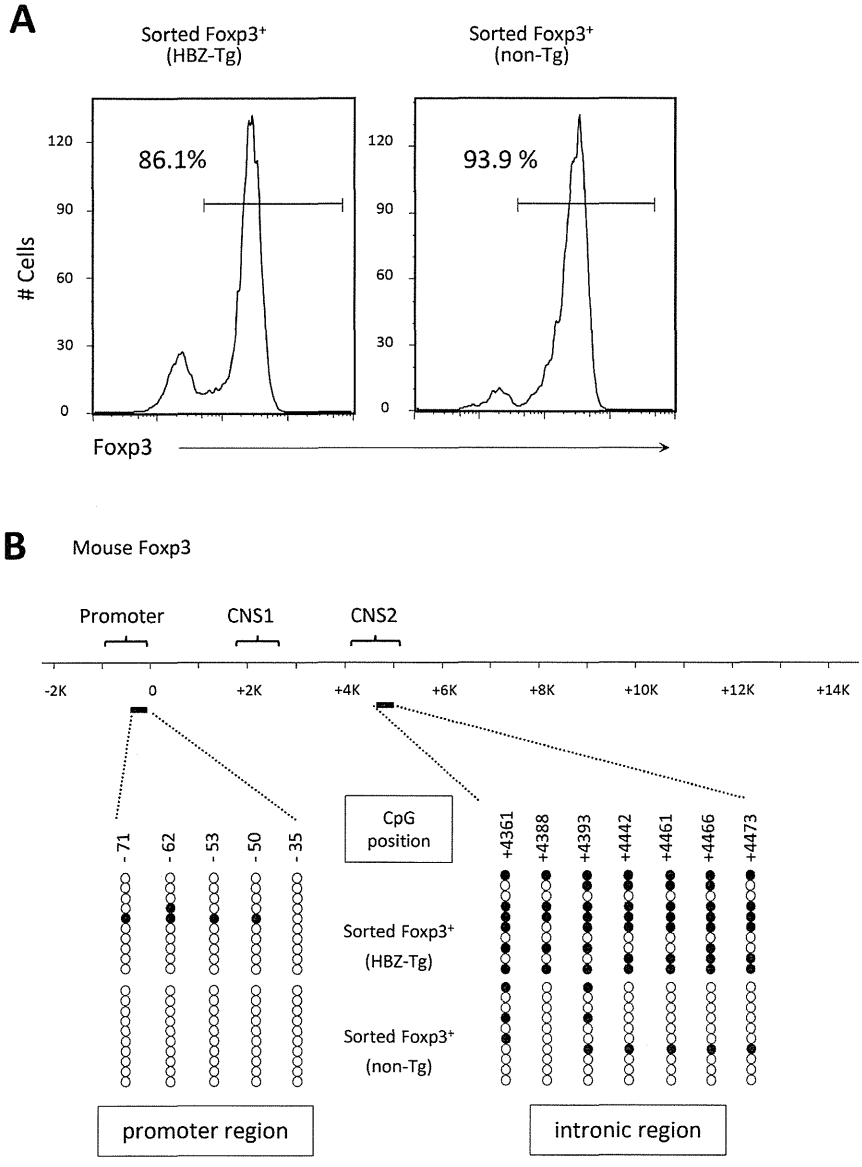

Figure 6. DNA methylation status in the promoter and intronic CpG island region of the *Foxp3* gene. (A) The purity of the isolated Treg cells, sorted from the spleens of male mice, was confirmed by staining the intracellular expression of Foxp3 and analysis by flow cytometry. (B) DNA methylation status in the indicated regions was determined by bisulfite sequencing. Each line represents one analyzed clone; open circles, unmethylated CpGs and filled circles, methylated CpGs.
doi:10.1371/journal.ppat.1003630.g006

possible mechanism of the increase in IFN-γ -producing Foxp3$^-$ T cells in HBZ-Tg mice. We reported that HBZ induced the *Foxp3* gene transcription via interaction with activation of TGF-β/Smad pathway [13]. Reduced expression of Foxp3 in HBZ-Tg CD4$^+$Foxp3$^-$ T cells might be caused by low HBZ expression in that cell population. To investigate this possibility, we analyzed the relationship between HBZ and Foxp3 expression in CD4$^+$ T cells of HBZ-Tg mice. We isolated CD4$^+$CD25$^+$GITR^{high} T cells as Foxp3$^+$ T cells, and CD4$^+$CD25$^-$GITR^{low} T cells as Foxp3$^-$ T cells from HBZ-Tg mice. Although Foxp3+ T cells are contaminated in CD4$^+$CD25$^-$GITR^{low} T cells, level of the Foxp3 gene transcript was much higher in CD4$^+$CD25^{high}GITR^{high} T cells (Figure S4). However, level of *HBZ* transcript was no different among these cells, indicating that level of HBZ expression is not associated with reduced Foxp3 expression.

Discussion

HTLV-1 is a unique human retrovirus with respect to its pathogenesis, since it causes not only a neoplastic disorder, but also various inflammatory diseases. For most viruses, tissue-damaging inflammation associated with chronic viral infection is generally triggered by the immune response against infected cells, which involves both antigen specific and non-specific T cells that produce pro-inflammatory cytokines, chemokines, and other chemical mediators that promote tissue inflammation [26]. However, this study shows that HTLV-1 can induce inflammation by a different mechanism that does not involve an immune response against infected cells, but instead, involves deregulation of CD4$^+$ T-cell differentiation mediated by HBZ. Since transgenic expression of HBZ does not induce an immune response to HBZ protein itself, the inflammation observed in this study is attributed to an intrinsic property of HBZ-expressing cells.

Studies of the pathogenesis of inflammatory diseases related to HTLV-1 are usually focused on HAM/TSP, since it is the most common inflammatory disease caused by this virus [9]. Two different mechanisms of HAM/TSP pathogenesis have been reported: one mechanism involves the immune response to viral antigens, and another mechanism implicates the proinflammatory attributes of HTLV-1-infected cells themselves. Previous studies reported a strong immune response to Tax in HTLV-1-infected individuals [9,27]. In lesions of the spinal cord, CD4$^+$ T cells expressing viral gene transcripts were identified by in situ hybridization [28]. The presence of CTLs targeting Tax in cerebrospinal fluid and lesions in the spinal cord suggest an important role of the immune response and the cytokines produced by CTLs in the pathogenesis of HAM/TSP by HTLV-1 [29]. Those studies showed the involvement of the immune response to Tax in the pathogenesis of HAM/TSP. In addition, cell-autonomous production of proinflammatory cytokines by HTLV-1-infected cells has been reported. HTLV-1-transformed cells produce a variety of cytokines, including IFN-γ, IL-6, TGF-ß, and IL-1α [30]. It was speculated that Tax was responsible for the enhanced production of these cytokines. In this study, we have shown a new role of HBZ in inflammatory diseases. CTLs against HBZ have been reported in HTLV-1 carriers and HAM/TSP patients; this immune response might be involved in inflammation caused by HTLV-1 [31]. However, an immune response to HBZ does not occur in HBZ-Tg mice, indicating that the proinflammatory phenotype of HBZ expressing T cells is sufficient to cause the inflammation.

Does HBZ induce IFN-γ production in CD4$^+$ T cells? HBZ and Tax have contradictory effects on many pathways. For example, Tax activates both the canonical and non-canonical NF-κB pathways, while HBZ suppresses the canonical pathway [32,33]. Conversely, HBZ activates TGF-ß/Smad pathway, while Tax inhibits it [13,34,35]. Tax activates the IFN-γ gene promoter, whereas HBZ suppresses the transcription of the IFN-γ gene through inhibition of AP-1 and NFAT, which are critical for IFN-γ gene transcription [36]. These findings collectively suggest that the enhanced production of IFN-γ is not due to a direct effect of HBZ, but may be attributed to the increased presence exFoxp3 T cells triggered by HBZ as shown in this study. Recent studies reported that exFoxp3 T cells produce higher amount of IFN-γ [17,37]. This indicates that increased production of IFN-γ in exFoxp3 T cells surpasses the suppressive function by HBZ. In this study, HBZ inhibited the production of TNF-α as we reported [36], indicating that enhanced production is specific to IFN-γ. However, it remains unknown how the production of IFN-γ is enhanced in exFoxp3 T cells.

We have shown that the Foxp3$^+$ T cells of HBZ-Tg mice tend to lose Foxp3 expression and change into IFN-γ-producing proinflammatory cells. This observation makes sense in the light of several other studies on Treg cells. It was reported thatFoxp3$^+$ T cells convert to Foxp3$^-$ T cells [37–39]. Recently, Miyao et al. reported that Foxp3 expression of peripheral T cells induced by activation is promiscuous and unstable, leading to conversion to exFoxp3 T cells [17]. Peripheral induced Foxp3$^+$ T cells show lower expression of CD25 and Helios, which corresponds to the phenotype we observed in the Foxp3$^+$ T cells of HBZ-Tg mice. Thus it is likely that HBZ induces unstable Foxp3 expression and generates iTreg cells, which then convert to exFoxp3 T cells with enhanced production of IFN-γ as shown in this study. It has recently been reported that CD4$^+$CD25$^+$CCR4$^+$ T cells in HAM/TSP patients were producing extraordinarily high levels of IFN-γ, when compared to cells of healthy donors. These findings are consistent with those of this study. Importantly, the frequency of these IFN-γ-producing CD4$^+$CD25$^+$CCR4$^+$Foxp3$^-$ T cells was increased and found to be correlated with disease severity in HAM/TSP patients [40]. In addition, it has been reported that HBZ expression is correlated with the severity of HAM/TSP [41]. Thus, the presence of abnormal HBZ-induced IFN-γ-producing cells is a plausible mechanism that leads to inflammation in HAM/TSP patients.

FOXP3 expression is detected in two thirds of ATL cases, suggesting that ATL cells originate from Treg cells in these cases [42,43]. Human FOXP3$^+$ T cells have been divided into three subgroups based on their functions and surface makers: resting Treg cells (rTreg), activated Treg (aTreg) cells, and FOXP3^{low}non-suppressive T cells [44]. Recently, we reported that HTLV-1 infection is frequently detected in Treg cells, which include FOXP3^{low} non-suppressive T cells and FOXP3^{high} activated Treg cells, and concordantly, some ATL cells also belong to the population of FOXP3^{low} non-suppressive T cells [44,45]. This suggests that HTLV-1 increases the population of aTreg and FOXP3^{low} non-suppressive T cells and induces leukemia/lymphoma of these cells. It is thought that most of nTreg are resting and activated Treg cells and iTreg cells contain both aTreg cells and Foxp3^{low} non-suppressive T cells in human. The CNS2 region in the Foxp3 locus is highly methylated in FOXP3^{low} non-suppressive T cells [44], like we report for the iTreg cells of HBZ-Tg mice. It is likely that a fraction of FOXP3^{low} non-suppressive T cells lose FOXP3 expression and change to FOXP3$^-$ proinflammatory T cells as reported in HAM/TSP patients [40], suggesting that the finding of this study is indeed the case in HTLV-1 infection.

It has been widely believed that nTreg cells represent a highly stable lineage in which few cells lose Foxp3 expression under normal homeostatic conditions [46]. In contrast, small subsets of CD25$^-$Foxp3$^+$ Treg cells have recently been reported to be unstable

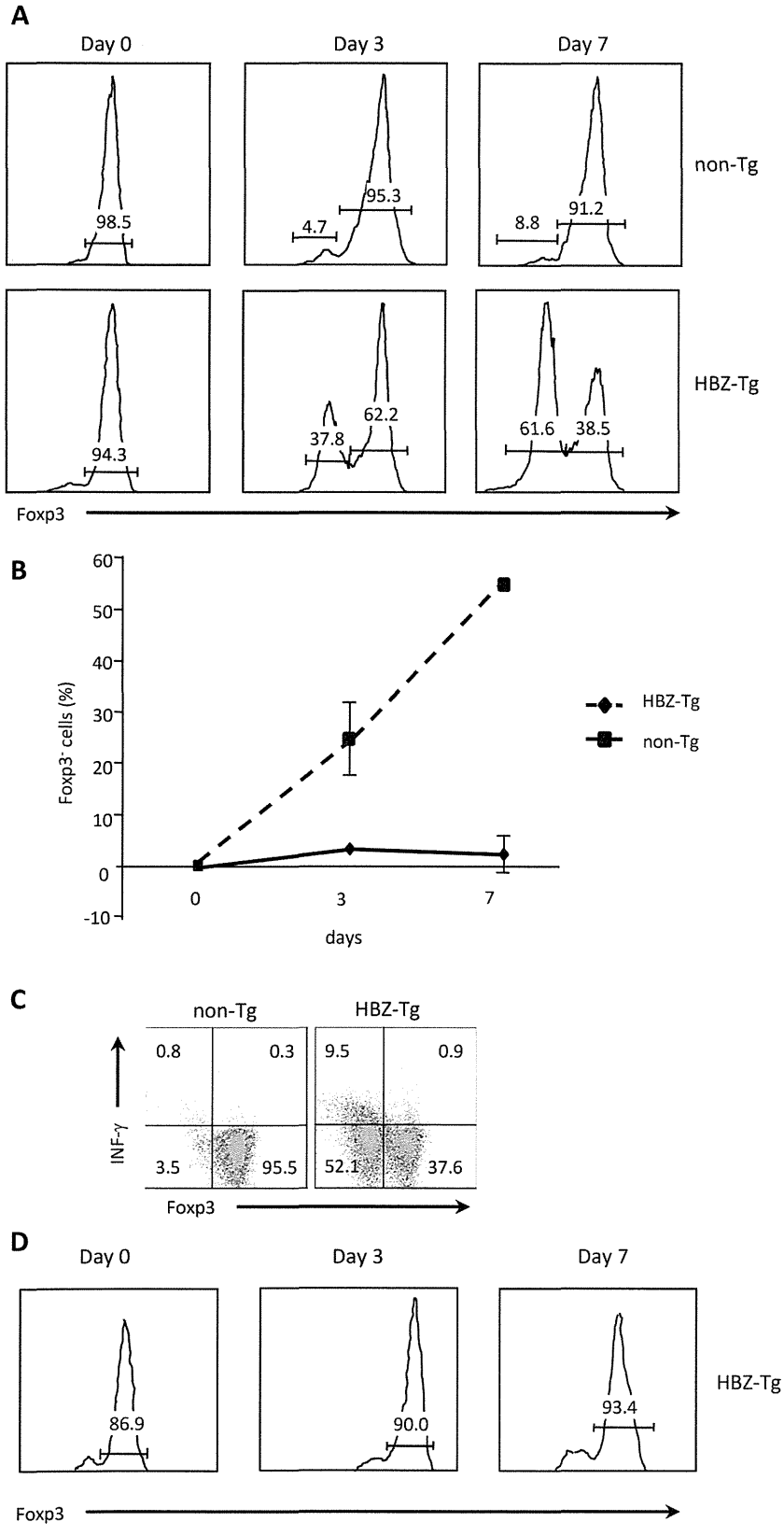

Figure 7. Stability of Foxp3 expression during *ex vivo* culture. (A) Treg cells, sorted from HBZ-Tg or non-Tg mice, were cultured in the presence of IL-2 for 3 or 7 days. The expression of Foxp3 was analyzed by flow cytometry. (B) Sequential changes of the Foxp3$^-$ population are shown. (C) IFN-γ production of *ex vivo* cultured Foxp3$^+$ cells was evaluated by intracellular staining. Sorted Treg cells were cultured for 7 days, and then stimulated for 4 h with PMA/ionomycin and protein transport inhibitor. (D) Foxp3 expression of sorted CD4$^+$CD25$^+$GITR^{high}thymocytes from HBZ-Tg mice.
doi:10.1371/journal.ppat.1003630.g007

and to rapidly lose Foxp3 expression after transfer into a lymphopenic host [16]. The CNS2 sequence is methylated in iTreg cells [24]. Consistent with this finding, CNS2 was heavily methylated in Treg cells of HBZ-Tg mice, indicating that Treg cells in HBZ-Tg mice largely belong to the iTreg cell subset. Foxp3 expression of $CD4^+$ thymocytes in HBZ-Tg mice did not decrease after *in vitro* culture, a fact which shows that loss of Foxp3 expression is not a direct effect of HBZ, but is due to the increased number of iTreg cells converting to exFoxp3 cells. Recently, it was reported that $Foxp3^+$ T cells without suppressive function convert to exFoxp3 T cells [17]. We recently reported that HBZ enhances *Foxp3* gene transcription by activating the TGF-ß/Smad pathway [13]. Collectively, it is likely that HBZ increases $Foxp3^+$ T cells in HBZ-Tg mice and most of $Foxp3^+$ T cells are iTreg and/or non-suppressive $Foxp3^+$ T cells. Foxp3 expression in HBZ-Tg mice is unstable as shown in this study, and such cells easily convert to exFoxp3 T cells, which produce excess amounts of IFN-γ, leading to inflammation.

Helios expression has been reported to be high in nTreg cells, and low in iTreg cells [20]. This study showed that Helios expression in $CD4^+Foxp3^+$ cells of HBZ-Tg mice was low although it was higher than control iTreg cells. Recently, it has been reported that stimulation enhances Helios expression of iTreg cells, which might account for increased Helios expression in $CD4^+Foxp3^+$ cells of HBZ-Tg mice compared with control iTreg cells [22]. In particular, inflammation caused by HBZ expression might increase Helios expression of iTreg cells of HBZ-Tg mice. In addition, it has been reported that Helios is not expressed in a part of nTreg cells and its expression is induced in iTreg cells, indicating that only Helios expression cannot discriminate nTreg cells from iTreg cells [21–23]. However, CNS2 is not methylated in $Helios^-$ nTreg cells, which shows that the methylation status of CNS2 is critical [21]. In this study, analysis of DNA methylation of CNS2 confirms that most of $CD4^+Foxp3^+$ cells in HBZ-Tg mice are iTreg cells. Importantly, the similar pattern of Heilos expression was observed in HAM/TSP patients.

The present study has demonstrated that HBZ-Tg mice develop inflammation in the intestines, skin and lungs. These tissues are always exposed to extrinsic antigens and commensal microbes, where Treg cells are critical for maintaining the homeostasis of the host immune system. In addition to the increased production of IFN-γ by HBZ-expressing cells, it is likely that the cell adhesion attributes of these cells also play a role in their pro-inflammatory phenotype. Treg cells express a variety of molecules that are important for cell adhesion, including LFA-1, CCR4, and CD103 [12]. We have shown that these molecules are also present on HBZ-expressing $CD4^+$ T cells. In this study, we showed that HBZ increases the number of iTreg cells, which subsequently convert into exFoxp3 T cells. The proinflammatory phenotype of HBZ-expressing T cells indicates that HBZ plays an important role in the inflammatory diseases caused by HTLV-1.

In conclusion, HBZ-Tg mice developed chronic inflammation accompanied with hyper IFN-γ production, which is consistent with the findings in HAM/TSP patients. $CD4^+Foxp3^+$ T cells, especially iTreg cells, were increased in HBZ-Tg mice. The expression of Foxp3 was not stable and tended to be lost, which resulted in the enhanced generation of exFoxp3 cells producing IFN-γ. This could be a mechanism for the development of chronic inflammation in HBZ-Tg mice and HTLV-1-infected individuals.

Materials and Methods

Mice and subjects

Transgenic mice expressing HBZ under the murine CD4 promoter have been previously described [12]. Genotypes were determined by means of PCR on mouse ear genomic DNA. All the mice were used at 10–20 weeks of age. Animal experimentation was performed in strict accordance with the Japanese animal welfare bodies (Law No. 105 dated 19 October 1973 modified on 2 June 2006), and the Regulation on Animal Experimentation at Kyoto University. The protocol was approved by the Institutional Animal Research Committee of Kyoto University (permit number: D13-02). All efforts were made to minimize suffering. A total of 10 HAM/TSP patients and 10 healthy donors participated in this study. Written informed consents were obtained from all the subjects in accordance with the Declaration of Helsinki as part of a clinical protocol reviewed and approved by the Institutional Ethics Committee of Kyoto University (approval number: 844). Blood samples were collected from the subjects and peripheral blood mononuclear cells (PBMC) were isolated by Ficoll-Paque Plus (GE Healthcare Bio-Sciences) density gradient centrifugation.

Adhesion of CD4+ T cells to immobilized ICAM-1

Production of recombinant mouse ICAM-1 was performed as described previously [47]. A 96-well plate was coated with 100 µl/well of 0.25 µg/ml mouse mICAM-1-Ig (R&D Systems) at 4°C overnight, followed by blocking with 1% BSA for 30 min. Mouse $CD4^+$ cells were labeled with 2′, 7′-bis-(2-carboxyethyl)-5-(and-6) carboxyfluorescein (Molecular Probes, Inc.), suspended in RPMI 1640 containing 10 mM HEPES (pH 7.4) and 10% FBS, transferred into the coated wells at 5×10^4 cells/well and then incubated at 37°C for 30 min. Non-adherent cells were removed by aspiration. Input and bound cells were quantitated in the 96-well plate using a fluorescence concentration analyzer (IDEXX Corp.).

Cell migration assay

Random cell migration was recorded at 37°C with a culture dish system for live-cell microscopy (DT culture dish system; Bioptechs). Thermoglass-based dishes (Bioptechs) were coated with 0.1 µg/ml mouse ICAM-1. $CD4^+$ mouse splenocytes were loaded in the ICAM-1-coated dish, and the dish was mounted on an inverted confocal laser microscope (model LSM510, Carl Zeiss MicroImaging, Inc.) Phase-contrast images were taken every 15 s for 10 min. The cells were traced and velocity was calculated using ImagePro^R Plus software (Media Cybernetics).

Flow cytometric analyses

Single-cell suspensions of mouse spleen, lung or PBMC or human PBMC were made in RPMI 1640 medium supplemented with 10% FBS. To detect Tax, $CD8^+$ cells were depleted from human PBMC using the BD IMAG cell separation system with the anti-human CD8 Particles-DM (BD Pharmingen) according to the manufacturer's directions and then the cells were cultured for 6 hours. Surface antigen expression was analyzed by staining with the following antibodies: anti-mouse CD4 (RM4-5), CD11a (2D7), CD18 (C71/16) or CD103 (M290) (all purchased from BD Pharmingen) or anti-human CD4 (RPA-T4), CD11a (HI111), CXCR3 (G025H7) (all purchased from BioLegend), CD18 (6.7), CD103 (Ber-ACT8) (all purchased from BD Pharmingen). For intracellular cytokine staining, cells were pre-stimulated with 20 ng/ml phorbolmyristate acetate (PMA, NacalaiTesque), 1 µM ionomycin (NacalaiTesque) and Golgi plug (BD Pharmingen) for 4 h prior to surface antigen staining. After this stimulation period, cells were fixed and permeabilized with Fixation/Permeabilization working solution (eBioscience) for 30 min on ice and incubated with antibodies specific for the following cytokines: IFN-γ (XMG 1.2), IL-17 (TC11-18H10), IL-2 (JES6-5H4) (all BD Pharmingen), TNF-α (MP6-XT22, eBioscience) and IL-4 (11B11, eBioscience).

Intracellular expression of mouse Foxp3 (FJK-16s, eBioscience), human FoxP3 (PCH101, eBioscience), Tax (MI73), human IFN-γ (4SB3, BD Pharmingen) and Helios (22F6, BioLegend) was detected following the protocol for cytokine staining. Dead cells were detected by pre-staining the cells with the Live/dead fixable dead cell staining kit (Invitrogen). Subsequently, the cells were washed twice, and analyzed by FACS CantoII with Diva software (BD Biosciences).

Histological analysis

Mouse tissue samples were either fixed in 10% formalin in phosphate buffer and then embedded in paraffin or frozen in embedding medium Optimal Tissue-TeK (SAKURA Finetek Japan). Hematoxylin and eosin staining was performed according to standard procedures. Tissue sections prepared from the frozen samples were also stained with anti-mouse IFN-γ (RMMG-1, Abcam), CD11a (M17/4, BioLegend), CD18 (N18/2, BioLegend), CD103 (M290, BD Pharmingen) and CD54 (ICAM-1)(YN1/1.7.4, BioLegend). Images were captured using a Provis AX80 microscope (Olympus) equipped with an OLYMPUS DP70 digital camera, and detected using a DP manager system (Olympus).

ELISA assay for chemokines

The α chemokines CXCL9 and CXCL10 were analyzed using an enzyme linked immunosorbent assay (ELISA). For α chemokines, capture and detection antibody concentrations were optimized using recombinant chemokines from R&D Systems Inc. (Minneapolis, MN, U.S.A.) according to the manufacturer's guidelines.

Direct sequencing after sodium bisulfite treatment

Genomic DNA was extracted from sorted Treg cells as described below. One mg of genomic DNA (10 μl) was denatured by the addition of an equal volume of 0.6 N NaOH for 15 min, and then 208 μl of 3.6 M sodium bisulfite and 12 μl of 1 mM hydroxyquinone were added. This mixture was incubated at 55°C for 16 hours to convert cytosine to uracil. Treated genomic DNA was subsequently purified using the Wizard clean-up system (Promega), precipitated with ethanol, and resuspended in 100 μml of dH_2O. Sodium bisulfite-treated genomic DNAs (50 ng) were amplified with primers targeting the specified DNA regions, and then PCR products were subcloned into the pGEM-T Easy vector (Promega) for sequencing. Sequences of 10 clones were determined for each region using Big Dye Terminator (Perkin Elmer Applied Biosystems) with an ABI 3100 autosequencer. The primers used for nested PCR were as follows:

for the mouse *Foxp3* promoter:
mproF, 5′-GTGAGGGGAAGAAATTATATTTTTAGATG-3′;
mproR, 5′-ATACTAATAAACTCCTAACACCCACC-3′;
mproF2, 5′-TATATTTTTAGATGATTTGTAAAGGGTAAA-3′;
mproR2, 5′-ATCAACCTAACTTATAAAAAACTACCACAT-3′.
For mouse *Foxp3* intronic CpG:
mintF, 5′-TATTTTTTTGGGTTTTGGGATATTA-3′;
mintR, 5′-AACCAACCAACTTCCTACACTATCTAT-3′;
mintF2, 5′-TTTTGGGTTTTTTTGGTATTTAAGA-3′;
mintR2, 5′-TTAACCAAATTTTTCTACCATTAAC-3′.

Sorting of Treg cells

To sort Treg cells, we isolated mouse splenocytes and resuspended them in FACS buffer for subsequent staining with the following antibodies purchased from BD Pharmingen: anti-mouse CD4 (RM4-5), GITR (DTA-1), CD25 (PC61). $CD4^+CD25^+GITR^{high}$ cells and $CD4^+CD25^-GITR^{low}$cells were sorted as $Foxp3^+$ or $Foxp3^-$cells using FACS AriaII with Diva software (BD Biosciences). To confirm the purity of the sorted Treg cells, we measured the percentage of Foxp3 expression by intracellular staining, as described above. Sorted Treg cells were cultured in RPMI1640 containing 10% FBS, antibiotics, and 50 μM 2-mercaptoethanol (Invitrogen).

Synthesis of cDNA and quantitative RT-PCR

Total RNA of sorted cells was extracted with TRIZOL reagent (Invitrogen) according to the manufacturer's instructions. Approximately 200 ng of RNA were used to prepare cDNA using the SuperScript III enzyme (Invitrogen). Levels of *HBZ* and *Foxp3* transcripts were determined with FastStart Universal SYBR Green Master reagent (Roche) in a StepOnePlus real time PCR system (Apllied Biosystems). Data was analyzed by the delta Ct method. The sequence of the primers used were as follows:

HBZ Forward: 5′-GGACGCAGTTCAGGAGGCAC-3′, Reverse: 5′-CCTCCAAGGATAATAGCCCG-3′; *Foxp3* Forward: 5′-CCCATCCCCAGGAGTCTTG-3′, Reverse: 5′-ACCATGACTAGGGGCACTGTA-3′; 18S rRNA Forward: 5′-GTAACCCGTTGAACCCCATT-3′, Reverse: 5′- CCATCCAATCGGTAGTAGCG -3′.

Supporting Information

Figure S1 Expression of CCR5 and CCR7 on $CD4^+$ T cells and production of CXCL9 and CXCL10 in HBZ-Tg mice. Expression of CCR5 (A) and CCR7 (B) on $CD4^+$ T cells was analyzed by flow cytometry. (C) CXCL9 (left) and CXCL10 (right) in sera of HBZ-Tg or non-Tg mice were measured by ELISA. The data shown mean ± SD of triplicates.
(PPTX)

Figure S2 Expression of Helios in $CD4^+Foxp3^+$ T cells in spleen and lung. Expression of Heilos of $Foxp3^+CD4^+$ T cells was analyzed in lungs (upper panels) and spleen (lower panels) from HBZ-Tg mice and non-Tg mice.
(PPTX)

Figure S3 Helios expression in thymocytes. Expression of Helios in $CD4^+$ $Foxp3^+$ cells of HBZ-Tg mouse (solid line) is compared to that of non-Tg mouse (dashed line) and isotype control (filled histogram). One representative result of three independent experiments is shown.
(PPTX)

Figure S4 HBZ expression is not correlated with Foxp3 expression in HBZ-Tg mice. (A) The proportion of $Foxp3^+$ cells in the Foxp3 (+) and Foxp3 (−) sorted populations was of 91.2% and 42.6%, respectively, when determined by intracellular staining. Expression of *HBZ* (B) and *Foxp3* (C) as measured by qRT-PCR in the sorted populations as described in material and methods. The expression level in whole CD4 cells from HBZ or WT mice were used as reference for *HBZ* and *Foxp3*, respectively.
(PPTX)

Acknowledgments

We thank Linda Kingsbury for kind revision of the manuscript.

Author Contributions

Conceived and designed the experiments: NYT YS MM. Performed the experiments: NYT YS PM KO KK. Analyzed the data: NYT YS TK MM. Contributed reagents/materials/analysis tools: MN. Wrote the paper: NYT YS PM KK TK MM.

References

1. Matsuoka M, Jeang KT (2007) Human T-cell leukaemia virus type 1 (HTLV-1) infectivity and cellular transformation. Nat Rev Cancer 7: 270–280.
2. Gessain A, Jouannelle A, Escarmant P, Calender A, Schaffar-Deshayes L, et al. (1984) HTLV antibodies in patients with non-Hodgkin lymphomas in Martinique. Lancet 1: 1183–1184.
3. Osame M, Usuku K, Izumo S, Ijichi N, Amitani H, et al. (1986) HTLV-I associated myelopathy, a new clinical entity. Lancet 1: 1031–1032.
4. Nakao K, Ohba N, Matsumoto M (1989) Noninfectious anterior uveitis in patients infected with human T-lymphotropic virus type I. Jpn J Ophthalmol 33: 472–481.
5. Mochizuki M, Yamaguchi K, Takatsuki K, Watanabe T, Mori S, et al. (1992) HTLV-I and uveitis. Lancet 339: 1110.
6. Sugimoto M, Nakashima H, Watanabe S, Uyama E, Tanaka F, et al. (1987) T-lymphocyte alveolitis in HTLV-I-associated myelopathy. Lancet 2: 1220.
7. LaGrenade L, Hanchard B, Fletcher V, Cranston B, Blattner W (1990) Infective dermatitis of Jamaican children: a marker for HTLV-I infection. Lancet 336: 1345–1347.
8. Morgan OS, Rodgers-Johnson P, Mora C, Char G (1989) HTLV-1 and polymyositis in Jamaica. Lancet 2: 1184–1187.
9. Matsuura E, Yamano Y, Jacobson S (2010) Neuroimmunity of HTLV-I Infection. J Neuroimmune Pharmacol 5: 310–325.
10. Satou Y, Yasunaga J, Yoshida M, Matsuoka M (2006) HTLV-I basic leucine zipper factor gene mRNA supports proliferation of adult T cell leukemia cells. Proc Natl Acad Sci U S A 103: 720–725.
11. Arnold J, Zimmerman B, Li M, Lairmore MD, Green PL (2008) Human T-cell leukemia virus type-1 antisense-encoded gene, Hbz, promotes T-lymphocyte proliferation. Blood 112: 3788–3797.
12. Satou Y, Yasunaga J, Zhao T, Yoshida M, Miyazato P, et al. (2011) HTLV-1 bZIP Factor Induces T-Cell Lymphoma and Systemic Inflammation In Vivo. PLoS Pathog 7: e1001274.
13. Zhao T, Satou Y, Sugata K, Miyazato P, Green PL, et al. (2011) HTLV-1 bZIP factor enhances TGF-{beta} signaling through p300 coactivator. Blood 118: 1865–1876.
14. Sakaguchi S, Yamaguchi T, Nomura T, Ono M (2008) Regulatory T cells and immune tolerance. Cell 133: 775–787.
15. Gavin M, Rudensky A (2003) Control of immune homeostasis by naturally arising regulatory CD4+ T cells. Current opinion in immunology 15: 690–696.
16. Zhou X, Bailey-Bucktrout SL, Jeker LT, Penaranda C, Martinez-Llordella M, et al. (2009) Instability of the transcription factor Foxp3 leads to the generation of pathogenic memory T cells in vivo. Nature immunology 10: 1000–1007.
17. Miyao T, Floess S, Setoguchi R, Luche H, Fehling HJ, et al. (2012) Plasticity of foxp3(+) T cells reflects promiscuous foxp3 expression in conventional T cells but not reprogramming of regulatory T cells. Immunity 36: 262–275.
18. Rubtsov YP, Niec RE, Josefowicz S, Li L, Darce J, et al. (2010) Stability of the regulatory T cell lineage in vivo. Science 329: 1667–1671.
19. Hori S, Nomura T, Sakaguchi S (2003) Control of regulatory T cell development by the transcription factor Foxp3. Science 299: 1057–1061.
20. Thornton AM, Korty PE, Tran DQ, Wohlfert EA, Murray PE, et al. (2010) Expression of Helios, an Ikaros transcription factor family member, differentiates thymic-derived from peripherally induced Foxp3+ T regulatory cells. Journal of immunology 184: 3433–3441.
21. Himmel ME, MacDonald KG, Garcia RV, Steiner TS, Levings MK (2013) Helios+ and Helios- cells coexist within the natural FOXP3+ T regulatory cell subset in humans. J Immunol 190: 2001–2008.
22. Gottschalk RA, Corse E, Allison JP (2012) Expression of Helios in peripherally induced Foxp3+ regulatory T cells. J Immunol 188: 976–980.
23. Akimova T, Beier UH, Wang L, Levine MH, Hancock WW (2011) Helios expression is a marker of T cell activation and proliferation. PLoS One 6: e24226.
24. Zheng Y, Josefowicz S, Chaudhry A, Peng XP, Forbush K, et al. (2010) Role of conserved non-coding DNA elements in the Foxp3 gene in regulatory T-cell fate. Nature 463: 808–812.
25. O'Shea JJ, Paul WE (2010) Mechanisms underlying lineage commitment and plasticity of helper CD4+ T cells. Science 327: 1098–1102.
26. Virgin HW, Wherry EJ, Ahmed R (2009) Redefining chronic viral infection. Cell 138: 30–50.
27. Bangham CR, Osame M (2005) Cellular immune response to HTLV-1. Oncogene 24: 6035–6046.
28. Moritoyo T, Reinhart TA, Moritoyo H, Sato E, Izumo S, et al. (1996) Human T-lymphotropic virus type I-associated myelopathy and tax gene expression in CD4+ T lymphocytes. Annals of neurology 40: 84–90.
29. Kubota R, Soldan SS, Martin R, Jacobson S (2002) Selected cytotoxic T lymphocytes with high specificity for HTLV-I in cerebrospinal fluid from a HAM/TSP patient. Journal of neurovirology 8: 53–57.
30. Dao T, Holan V, Minowada J (1993) Multiple and heterogeneous patterns of cytokine production in 18 leukemia and in vitro transformed mature T cell lines reflect the individuality of human leukemias. International journal of hematology 57: 139–146.
31. Macnamara A, Rowan A, Hilburn S, Kadolsky U, Fujiwara H, et al. (2010) HLA class I binding of HBZ determines outcome in HTLV-1 infection. PLoS Pathog 6: e1001117.
32. Sun SC, Yamaoka S (2005) Activation of NF-kappaB by HTLV-I and implications for cell transformation. Oncogene 24: 5952–5964.
33. Zhao T, Yasunaga J, Satou Y, Nakao M, Takahashi M, et al. (2009) Human T-cell leukemia virus type 1 bZIP factor selectively suppresses the classical pathway of NF-kappaB. Blood 113: 2755–2764.
34. Arnulf B, Villemain A, Nicot C, Mordelet E, Charneau P, et al. (2002) Human T cell lymphotropic virus oncoprotein tax represses TGF-{beta}1 signaling in human T cells via c-Jun activation: a potential mechanism of HTLV-I leukemogenesis. Blood 100:4129–38.
35. Lee DK, Kim BC, Brady JN, Jeang KT, Kim SJ (2002) Human T-cell Lymphotropic Virus Type 1 Tax Inhibits Transforming Growth Factor-beta Signaling by Blocking the Association of Smad Proteins with Smad-binding Element. J Biol Chem 277: 33766–33775.
36. Sugata K, Satou Y, Yasunaga J, Hara H, Ohshima K, et al. (2012) HTLV-1 bZIP factor impairs cell-mediated immunity by suppressing production of Th1 cytokines. Blood 119: 434–444.
37. Yang XO, Nurieva R, Martinez GJ, Kang HS, Chung Y, et al. (2008) Molecular antagonism and plasticity of regulatory and inflammatory T cell programs. Immunity 29: 44–56.
38. Komatsu N, Mariotti-Ferrandiz ME, Wang Y, Malissen B, Waldmann H, et al. (2009) Heterogeneity of natural Foxp3+ T cells: a committed regulatory T-cell lineage and an uncommitted minor population retaining plasticity. Proc Natl Acad Sci U S A 106: 1903–1908.
39. Xu L, Kitani A, Fuss I, Strober W (2007) Cutting edge: regulatory T cells induce CD4+CD25-Foxp3- T cells or are self-induced to become Th17 cells in the absence of exogenous TGF-beta. Journal of immunology 178: 6725–6729.
40. Yamano Y, Araya N, Sato T, Utsunomiya A, Azakami K, et al. (2009) Abnormally high levels of virus-infected IFN-gamma+ CCR4+ CD4+ CD25+ T cells in a retrovirus-associated neuroinflammatory disorder. PLoS One 4: e6517.
41. Saito M, Matsuzaki T, Satou Y, Yasunaga J, Saito K, et al. (2009) In vivo expression of the HBZ gene of HTLV-1 correlates with proviral load, inflammatory markers and disease severity in HTLV-1 associated myelopathy/tropical spastic paraparesis (HAM/TSP). Retrovirology 6: 19.
42. Karube K, Ohshima K, Tsuchiya T, Yamaguchi T, Kawano R, et al. (2004) Expression of FoxP3, a key molecule in CD4CD25 regulatory T cells, in adult T-cell leukaemia/lymphoma cells. Br J Haematol 126: 81–84.
43. Chen S, Ishii N, Ine S, Ikeda S, Fujimura T, et al. (2006) Regulatory T cell-like activity of Foxp3+ adult T cell leukemia cells. Int Immunol 18: 269–277.
44. Miyara M, Yoshioka Y, Kitoh A, Shima T, Wing K, et al. (2009) Functional delineation and differentiation dynamics of human CD4+ T cells expressing the FoxP3 transcription factor. Immunity 30: 899–911.
45. Satou Y, Utsunomiya A, Tanabe J, Nakagawa M, Nosaka K, et al. (2012) HTLV-1 modulates the frequency and phenotype of FoxP3+CD4+ T cells in virus-infected individuals. Retrovirology 9: 46.
46. Curotto de Lafaille MA, Lafaille JJ (2009) Natural and adaptive foxp3+ regulatory T cells: more of the same or a division of labor? Immunity 30: 626–635.
47. Kinashi T, Katagiri K (2005) Regulation of immune cell adhesion and migration by regulator of adhesion and cell polarization enriched in lymphoid tissues. Immunology 116: 164–171.

厚生労働科学研究費補助金
難病・がん等の疾患分野の医療の実用化研究事業（がん関係研究分野）
「成人T細胞白血病の治癒を目指した病因ウイルス特異抗原を
標的とする新規複合的ワクチン療法：
抗CCR4抗体を併用した樹状細胞療法 第I/II相試験」
（平成25年度　総括・分担研究報告書）

発行日　平成２６年３月

発　行　国立病院機構九州がんセンター
福岡市南区野多目３－１－１（〒811-1395）
TEL 092（541）３２３１
FAX 092（551）４５８５
http://www.ia-nkcc.jp/

印　刷　陽文社印刷株式会社
〒815-0082 福岡市南区大楠2丁目4番10号
TEL(092)522-0081 FAX(092)522-0273